Petrological and geochemical studies of Tonaru epidote-amphibolite and surrounding schists in the Sanbagawa metamorphic belt, central Shikoku

四国中央部三波川変成帯東平緑れん石-角閃岩及び周囲の片岩の岩石学的・地球化学的研究

HUANG SHUAIMIN

A dissertation for the degree of Doctor of Science

Department of Earth and Environmental Sciences,

Graduate School of Environmental Studies, Nagoya University

（名古屋大学大学院環境学研究科地球環境科学専攻

学位論文　博士　（理学）　）

ABSTRACT

The Sanbagawa metamorphic belt in Southwest Japan, one of the most famous metamorphic belts in the world, is a typical subduction-type low-temperature, high-pressure metamorphic belt, and this metamorphic belt extends for about 800 km, stretching from the Kanto mountains, through Shikoku including the Besshi region, central shikoku, discussed in this paper, to the Kyushu island (Fig. 1a).

The Sanbagawa metamorphic belt in Shikoku has been studied in detail for a long time, because of the wide and good exposure and systematic variations in metamorphic facies from the pumpellyite-actinolite, blueschist-greenschist transition, epidote-amphibolite, to amphibolite facies (e.g., Banno, 1964; Banno *et al.*, 1978; Enami, 1982; Banno and Sakai, 1989). It is widely accepted that the Sanbagawa metamorphic belt in Southwest Japan is derived from a Cretaceous subduction complex of the East Asian continental margin (Isozaki and Itaya 1990; Wallis, 1998). The high-grade part of this belt is developed in central Shikoku, where the belt has been divided into four metamorphic zones based on the paragenesis of metapelite: the chlorite, garnet, albite-biotite and oligoclase-biotite zones, in ascending order of metamorphic grade (Higashino, 1990). The Tonaru amphibolite mass occurs in the oligoclase or albite-biotite zones (Miyagi, 2000).

The Sanbagawa metamorphic rocks widely occur in the Besshi region of central Shikoku (Fig. 1b), and have been studied over 40 years on geology, petrology, geochemistry and geochronology by many workers (e.g., Banno, 1964, Banno *et al*., 1978; Enami, 1982; Itaya and Takasugi, 1988; Okamoto *et al*., 2000). The Tonaru mass (6.5 km × 1 km) is one of the eclogite-bearing bodies located in the western part of the Besshi region (Fig. 1b). The Tonaru mass mainly consists of epidote-amphibolite

with minor eclogites (Miyagi, 2000). Protoliths of these lithologies have been considered to be gabbro and its equivalence. However, metamorphosed limestone layer occurs in the Tonaru mass, suggesting a possibility that a part of The Tonaru mass is not metagabbro but metasedimentary sequence. The outcrops of the Tonaru epidote-amphibolites are well observed along the Kokuryo-gawa (Kokuryo River). Therefore, It is regarded as a suitable area for a study on their relationships between the Tonaru epidote-amphibolite rock and the surrounding rocks such as Sanbagawa pelitic schist, and Sanbagawa basic schist.

The author studied the the Tonaru epidote-amphibolite, the published whole-rock chemical compositions of Iratsu epidote amphibolite, Seba amphibolite, Sanbagawa basic schist, and metapelite collected from the same region (Besshi region) will be used for comparison. The main objectives of this study are as follows:

(1) Conduct a study on the geochemical and petrological characteristics of the Tonaru epidote-amphibolite, and surrounding schists (Sanbagawa metapelite, Sanbagawa basic schist) along the Kokuryo River in the Besshi region of central Shikoku;

(2) Compare the Tonaru epidote-amphibolite with the other amphibolite mass in the Besshi region, for example, Iratsu epidote-amphibolite, and Seba eclogitic basic schist, and compare the Tonaru epidote-amphibolite with surrounding schists, for example, Sanbagawa metapelite, and Sanbagawa basic schist. along the the Kokuryo River in the Besshi region of central Shikoku;

(3) Discuss the origin of the protoliths of the Tonaru epidote-amphibolite.

The Tonaru epidote-amphibolite is one of the largest metagabbro dominated bodies occurring in schistose lithologies of the Sanbagawa metamorphic belt, central Shikoku.

Geochemical study (major and trace elements, including rare earth elements (REEs)), in the Tonaru epidote-amphibolite and surrounding basic schists and metapelites along the Kokuryo River in the Besshi region of central Shikoku have been systematically investigated, material interactions at their lithologic boundaries are discussed in this paper.

Most parts of the Tonaru epidote-amphibolite have petrographic and geochemical characteristics similar to the other epidote-amphibolites (Iratsu epidote-amphibolites) and basic shicst in the Besshi region, which are derived from the gabbro. On the other hand, some of the epidote-amphibolites, which were collected from the southern and northern margins of the Tonaru body, show SiO_2-rich ($SiO_2 > 60\%$) compositions. On the other hand, some of the epidote-amphibolites show intermediate compositions between the basic schist and pelitic schist in the SiO2–FeO*/MgO, Al_2O3–CaO/(CaO + Na_2O + K_2O), Ti/100-Zr-Sr/2, and V-Ba systems, and have light REE-enriched patterns similar to that in the sedimentary lithologies, and are sometimes richer in some trace elements, for example, Ni, Co, and Cr , which implies that parts of the Tonaru body are probably affected by ultramafic materials.

According to these data, the protoliths of the Tonaru epidote-amphibolites could be grouped into 2 types : (1) a gabbroic lithology; and (2) sedimentary mixtures of mafic, ultramafic and/or pelitic materials, likely derived from an oceanic island arc. There is no apparent compositional modification detected at a shear zone of 1.5–2.5 m width that developed at the northern boundary between the Tonaru epidote-amphibolite and metapelite. This feature implies that lithological mixing at this boundary was relatively insignificant during metamorphism and might not have effectively altered compositions

of the metamorphic rocks without element transport promoted by circulating metamorphic fluids.

Keywords: lithological mixing, metagabbro, schist, subduction zone, Sanbagawa belt

1. INTRODUCTION

Subduction zones are plate tectonic boundaries where two tectonic plates meet, and one plate is thrust beneath the other plate. This process results in a geohazard, such as volcanoes and earthquakes. On the other hand, Subduction zones also provide an unique environment where various materials such as sedimentary rocks, and mafic-ultramafic lithologies derived from the crust and mantle wedge, respectively, encounter to each other. Therefore, it could be inferred that mechanical (physical) and chemical interactions have dynamically progressed during the subduction process along the interface between the subducted slab and the crust-mantle zone beneath an arc-trench system (Planka and Langmuir, 1998; Stern, 2002). Mechanical and/or sedimentary processes relating to protolith formation of metamorphic rocks before subduction might also promote modifications in rock composition.

In the Besshi region of the Sanbagawa metamorphic belt in central Shikoku, SouthWest Japan (Fig. 1b), there are extensive occurrences of various types of metamorphic rocks that have originated from different protoliths of peridotite, gabbro, basalt, shale-sandstone, and limestone, and the contact relationships between these different lithologies have been well documented (Onuki *et al.*, 1978; Moriyama, 1990; Aoya, 2001; Kugimiya and Takasu, 2002; Aoya *et al*., 2006; Sakurai and Takasu, 2009; Endo *et al.*, 2015). For example, Moriyama (1990) and Sakurai and Takasu (2009) reported lithified fracture zones (10–30 cm in width) and chlorite-rich and talc-bearing lithologies (5–50 cm in width) at the boundaries between metamorphosed layered gabbro (epidote-amphibolite) and sediment (pelitic schist), respectively. Aoya *et al*. (2006) also described siliceous shear zones of 0.3–7.4 m width at the boundary between metagabbro and the surrounding schists. As such, the Besshi region is one of the best

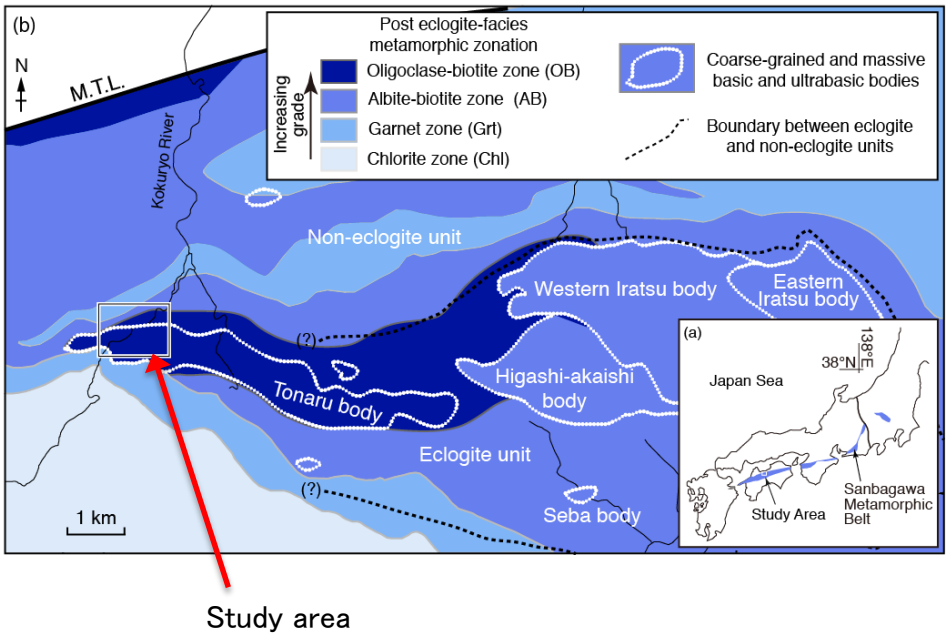

(c)

Fig. 1. (a) Index map of the Sanbagawa belt. (b) Metamorphic zone map of the Sanbagawa metamorphic belt in the Besshi reigon. (c) Outcrop of Tonaru epidote-amphibolite.

(a)

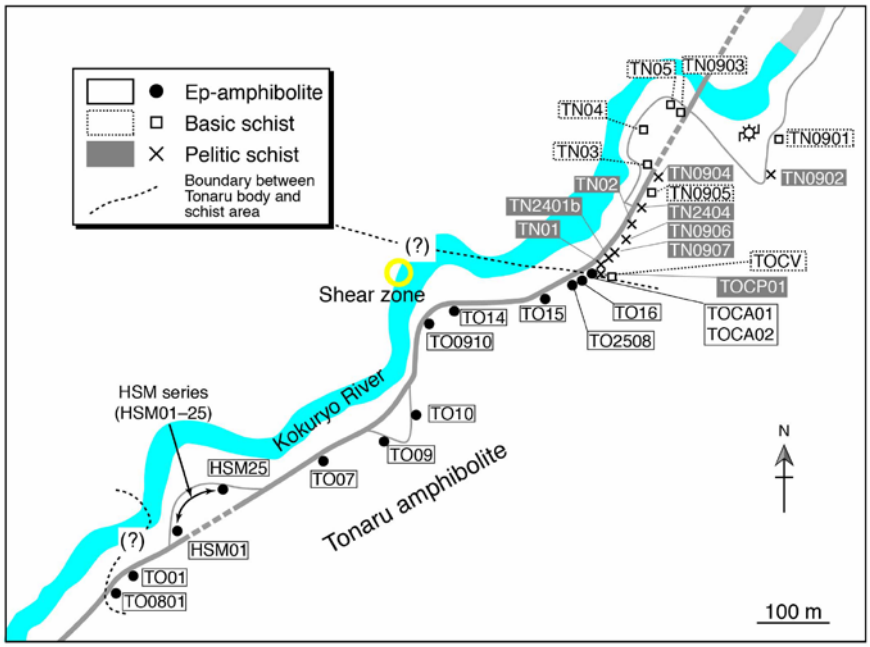

(b)

(c)

Fig. 2. (a) Locality map of the epidote-amphiblite, schist samples along the kokuryo river. (b) Outcrop of thin pelitic lenses (1–3 m in thickness) near the northern margin and (c) A layer of marble also occurs in the southern part of the Tonaru body.

subduction-zone metamorphic belts that documents a characteristic succession of lithologies from the ridge-trench system, and allows for analysis of the material and chemical interactions of various components during subduction.

Field relationships between the Tonaru epidote-amphibolite body and surrounding metapelites and basic schists are well exposed along the Kokuryo River in the Tonaru area of the Sanbagawa belt in the Besshi region (Fig. 1b, c). Miyagi and Takasu (2005) reported the occurrence of thin pelitic lenses (1–3 m in thickness) (Fig. 2a, b), which located in northern margin of intercalated within the epidote-amphibolites at the southern part of the Tonaru body. The epidote-amphibolites around these lenses are significantly more siliceous (SiO_2 > 65 wt%) than other common epidote-amphibolites. A layer of marble (Fig. 2c) also occurs in the southern part of the Tonaru body (Banno *et al.*, 1976; Wada *et al.*, 1986). However, the petrological and geochemical characteristics of the epidote-amphibolites, including these pelitic lenses and marble layer, and their origins, have not yet been discussed in detail. This study mainly documents the petrographic, mineralogical characteristics and variations in whole-rock compositions of the Tonaru epidote-amphibolite along the Kokuryo River as a case study on the interaction and compositional modifications at the interface between compositionally different lithologies. Furthermore, the mechanical and chemical interactions during the formation of protoliths and their recrystallization in a subduction zone are also discussed.

2. GEOLOGICAL SETTING

The Sanbagawa metamorphic belt is a typical subduction-type metamorphic belt, and extends over 800 km from the Kanto Mountains in the east to eastern Kyushu in the

west. To the north, it is separated from the Cretaceous high-temperature type Ryoke Belt by the Median Tectonic Line, the major strike-slip fault dividing southwest Japan into the Inner Zone of the continental region and Outer Zone of the Pacific Ocean side (Fig. 1a). The Sanbagawa metamorphic rocks widely occur in the Besshi region of central Shikoku (Fig. 1b), and have been studied over 40 years on geology, petrology, geochemistry and geochronology by many workers (e.g., Banno., 1964, Banno *et al*., 1978; Enami, 1982; Itaya and Takasugi, 1988; Okamoto *et al*., 2000).

The Cretaceous Sanbagawa metamorphic belt is one of the best-documented low-temperature, high-pressure subduction type regional metamorphic belts in the world (Banno, 2004; Wallis and Okudaira, 2016). This belt has a maximum width of about 30 km in central Shikoku and is well exposed in the Besshi region. The high-grade part of this belt is developed in central Shikoku, in which the belt has been divided into four metamorphic zones based on the paragenesis of metapelite: the chlorite, garnet, albite-biotite and oligoclase-biotite zones, in ascending order of metamorphic grade (Enami, 1982; Higashino, 1990). Metabasic lithologies in the albite-biotite and oligoclase-biotite zones have mineral assemblages that include barroisite/hornblende/pargasite + epidote + sodic plagioclase + quartz ± garnet ± muscovite, and their metamorphic grade roughly coincides with that of the epidote-amphibolite facies. Pressure and temperature conditions of these two mineral zones were estimated as 0.8–1.1 GPa and 470–635 °C, respectively (Enami, 1983; Enami *et al.*, 1994; Wallis *et al.*, 2000).

Variously sized bodies of peridotite, serpentinite, and metagabbro-dominated lithologies occur sporadically within the schistose area that consists of metapelite, metabasalt, and metachert in the Besshi region of the Sanbagawa Belt (Fig. 1b). The

Higashi-akaishi peridotite, the largest ultramafic body within the Sanbagawa Belt, together with the related serpentinite, originated from the interior of the mantle wedge, most likely the forearc upper mantle (Hattori *et al.*, 2010). The Iratsu epidote-amphibolite body is the largest metagabbro-dominated body in the Sanbagawa Belt and was divided into eastern and western regions. The Eastern Iratsu body is composed of metagabbro, while the Western Iratsu body consists mainly of metagabbro, metabasalt, and marble (Kugimiya and Takasu, 2002; Terabayashi *et al.*, 2005; Endo and Tsuboi, 2013). Protoliths of large parts of the Iratsu body are likely derived from the middle-lower crust of an ocean island arc (Utsunomiya *et al.*, 2011).

Metagabbro-dominant bodies such as the Iratsu body are massive and relatively coarser-grained than the surrounding schistose rocks and are conventionally referred to as amphibolite or epidote-amphibolite to distinguish their lithological features. Major schistose basic and pelitic lithologies around the epidote-amphibolite bodies are referred to as basic and pelitic schists and were derived mainly from mid-ocean ridge basalt (MORB) (Okamoto *et al.*, 2000; Nozaki *et al.*, 2006; Uno *et al.*, 2014) and continental materials (Utsunomiya *et al.*, 2011), respectively.

Lines of evidence for eclogite facies equilibrium, which developed prior to prograde epidote-amphibolite facies metamorphism, are sometimes retained in the epidote-amphibolites (Takasu, 1984; Aoya, 2001; Ota *et al.*, 2004; Miyagi and Takasu, 2005; Miyamoto *et al.*, 2007; Endo, 2010; Endo and Tsuboi, 2013) and surrounding schists (Naohara and Aoya, 1997; Sakurai and Takasu, 2009; Kouketsu and Enami, 2010; Kouketsu *et al.*, 2010). Therefore, the Besshi region is divided into eclogite and non-eclogite units (Wallis and Aoya, 2000; Mouri and Enami, 2008; Kouketsu *et al.*,

2014) (Fig. 1b). The distribution of eclogite unit was also reported from the Asemi-gawa (Asemi River: Taguchi and Enami, 2014) and Kotsu–Bizan (Matsumoto *et al.*, 2003; Tsuchiya and Hirajima, 2013; Kabir and Takasu, 2016) regions, which are located about 20 km southwest and 80–110 km east of the Besshi region, respectively. Lithologies of the eclogite unit have experienced a successive metamorphic *P-T* path from prograde eclogite facies stage to decompression and hydration reaction stage which was further followed by a retrograde epidote–amphibolite facies stage (Fig. 3; Aoya, 2001; Zaw Win Ko *et al.*, 2005; Wallis *et al.*, 2009; Kouketsu *et al.*, 2014; Enami *et al.*, 2017). In contrast, the non-eclogite units record a simple clockwise *P-T* path consisting of prograde stage up to the epidote–amphibolite facies and subsequent retrograde stages.

The Tonaru epidote-amphibolite body investigated in this study is 6.5 × 1 km in area and is exposed in the western part of the Besshi region (Fig. 1b). This body and the surrounding schists have been geologically and petrologically documented by Moriyama (1990), Miyagi and Takasu (2005), Matsuura *et al.* (2013), and Kabir *et al.* (2016). The Tonaru body belongs to the eclogite unit, and thus, has experienced two prograde metamorphic stages of eclogite facies and subsequent epidote-amphibolite facies, with *P-T* conditions estimated at ≥ 1.5 GPa/700–730 °C (Miyagi and Takasu, 2005) and 0.9–1.1 GPa/585–635 °C (Enami, 1983; Enami *et al.* 1994; Wallis *et al.*, 2000), respectively. Moriyama (1990) divided the Tonaru body into epidote-amphibolite and diopside-amphibolite. The epidote-amphibolite, which is the dominant lithology of the Tonaru body, is usually composed of alternating mafic and felsic layers of various widths (Fig. 4a) and sometimes shows coarse grained and granular texture. The diopside-amphibolite shows banded structure consisting of pale

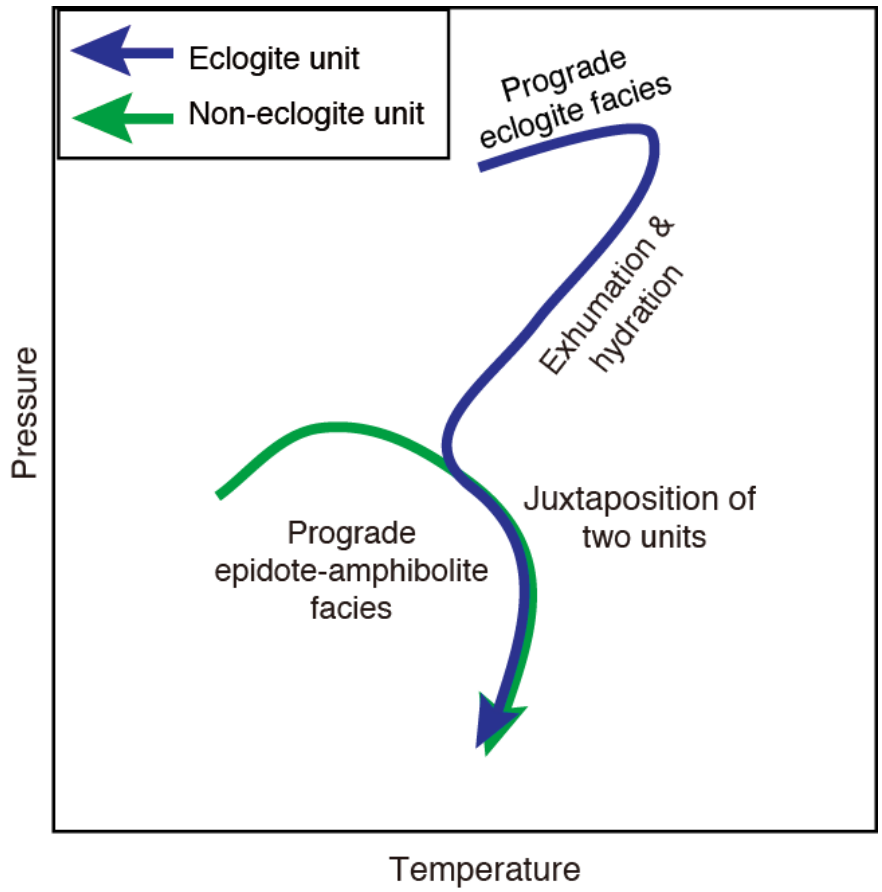

Fig. 3. Schematic diagram showing the pressure-temperature-time (*P-T-t*) paths of the eclogite and non-eclogite units of the Sanbagawa belt [partly modified from Fig. 6b of Suzuki et al. (2018)]. Abbreviations: O04, Okamoto *et al*. (2004); A09, Aoki *et al*. (2009); W09, Wallis *et al*. (2009); I11. Itaya *et al*. (2011); S18, Suzuki *et al*. (2018).

greenish diopside-rich bands and dark greenish amphibole-rich bands. Banno *et al.* (1976), Kunugiza *et al.* (1986), Takasu (1989) and many other researchers considered that the mafic and felsic layers of the epidote-amphibolite were originally pyroxene- and calcic plagioclase-rich parts of the layered gabbro, respectively, whereas diopside-amphibolite was probably metamorphosed mafic cumulate. Therefore, the protoliths of amphibolites are considered to have been gabbroic lithologies. However, a layer of marble (0.3–0.8 m in width) is intercalated concordantly or subconcordantly in the host epidote-amphibolite near the southern margin (Fig. 4b). Wada *et al.* (1984) showed that the marble in the Tonaru body had initial $^{87}Sr/^{86}Sr$ (0.70697 ± 0.00016) when the marble was formed and $\delta^{13}C$ PDB (1.6–2.8 ‰ PDB) values similar to the carbonates in the metapelites and quartz schists (0.70705 ± 0.00016 to 0.70804 ± 0.00024 and -1.6–2.1 ‰ PDB). Thus, they hypothesized that the Tonaru marble was probably derived from sedimentary carbonates and/or carbonates re-equilibrated with metamorphic fluid segregated from crystalline schists during the Sanbagawa metamorphism. Quartz-rich veins or layers, which are strongly folded with the surrounding amphibole-rich parts, developed near the southern margin of the Tonaru epidote-amphibolite body (Fig. 4c, d). Thin pelitic lenses (1–3 m in thickness) (Fig. 2a), was observeed in northern margin of intercalated within the epidote-amphibolites at the southern part of the Tonaru body. Kouketsu *et al.* (2014) reported an investigation of the composite metamorphic history recorded in garnet porphyroblasts from the metapelites and also discussed the distribution of eclogite facies lithologies in the Besshi region, Central Shikoku, southwest Japan.

The samples studied were collected from a route along the Kokuryo River, which traverses the boundary between the Tonaru epidote-amphibolite and the surrounding

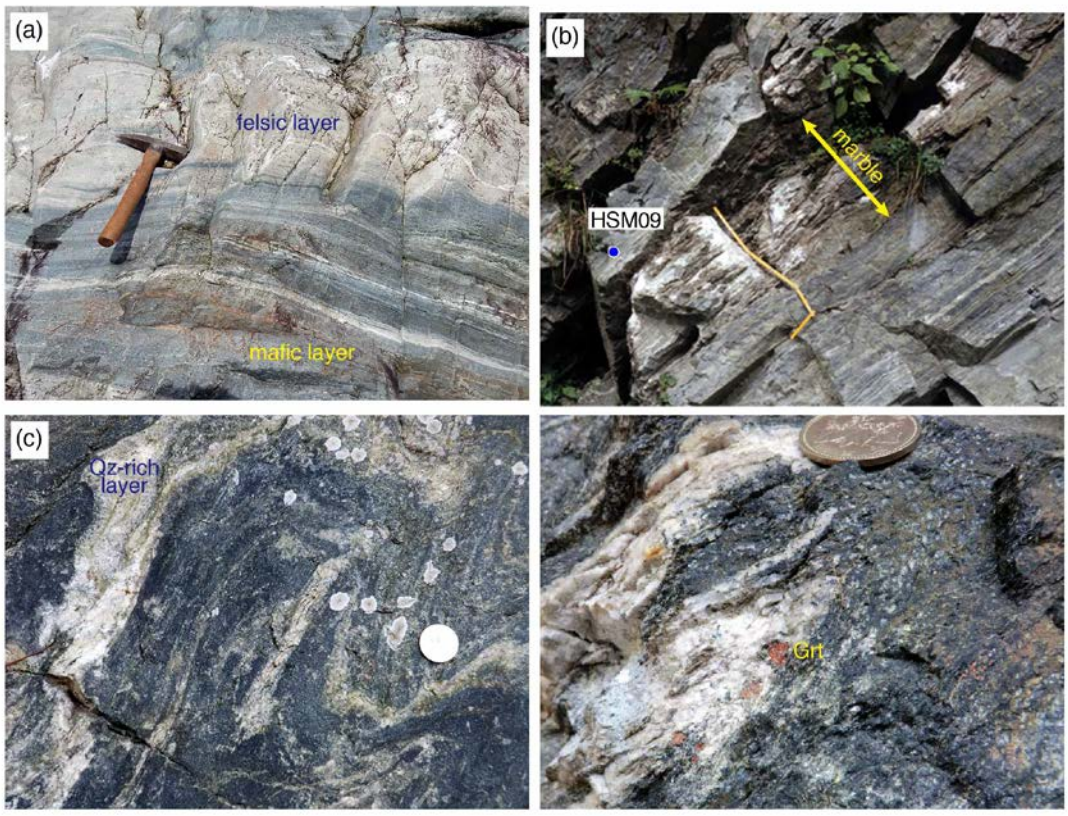

Fig. 4. Photographs of representative outcrops of the Tonaru epidote-amphibolite: (a) layered metagabbro showing alternating amphibole-rich and felsic layers near the location of sample TO10, (b) a layer of marble intercalated concordantly or subconcordantly in host epidote-amphibolite (the location of sample HSM09), (c) well-foliated amphibole-rich lithology having quartz-rich veins or layers (near the locations of sample HSM03a and b), and (d) garnet-bearing epidote-amphibolite foliated amphibole-rich lithology having quartz-rich veins or layers (near the (near the location of sample HSM02).

schists (Fig. 2a). Most parts of the Tonaru epidote-amphibolite (TO series in Fig. 2a) show a typical layered metagabbro texture (Fig. 4a: cf. Banno *et al.*, 1976). However, samples collected near the southern margin (HSM series in Fig. 2a) show distinctive textural varieties; some samples are amphibole-rich and massive (Fig. 4c, d), whereas others consist of alternating thin (< 2–3 cm in width), amphibole-rich and felsic layers (Fig. 4b) all of which belong to the oligoclase-biotite zone (Enami, 1982). The field relationship between the epidote-amphibolite and schists on the southern side was not directly observed on the trail and riverbed along the Kokuryo River. However, Hara *et al.* (1990) and Moriyama (1990) reported that the schists lie in a fault contact along the southern boundary of the Tonaru epidote-amphibolite. On the northern side of the Tonaru epidote-amphibolite, a shear zone of 1.5–2.5 m width developed along the boundary between the epidote-amphibolite and metapelite (Fig. 2a). The shear zone consists of a basic layer on the Tonaru body side and fine alternating basic and pelitic bands of mm–cm thickness on the pelitic schist side. Samples TOCA01 and 02 were obtained from the basic layer. Basic (TOCV) and pelitic (TOCP01) lenses (up to 5 cm in thickness) are locally distributed in the matrices of basic and pelitic alternating layers.

3. PETROGRAPHY

In the Besshi region, petrological characteristics of fourty-three samples from the Tonaru amphibolite, four samples from the shear zone, and fourteen samples from the schistose area collected along the Kokuryo River were studied (Fig. 2a). Mineral assemblages of the epidote-amphibolites and modal compositions of some selected samples are listed in Table 1.

TO (Tonaru) series were collected from central part of the Tonaru body, and Sample TO10 (Figs. 5a), is mainly composed of amphibole (hornblend), quartz, epidote, sodic plagioclase, with minor Titanite, rutile. Compared to the other common HSM amphibolite samples, there are no significant difference in mineral assemblage.

HSM (Huang Shuaimin) series were collected from the southern margin of the Tonaru amphibolite. Sample HSM03b (Fig. 4b), which was collected from the southernmost part of the Tonaru mass, and is mainly composed of amphibole (hornblend), epidote, muscovite, chlorite, sodic plagioclase, and quartz, with minor amounts of garnet, rutile, apatite, and opaque. Garnet locally occurs as anhedral grains, primarily located at the southern and northern margins of the body (Fig. 8a, b, c), and in Sample HSM03b, a lot of garnets were observed. Chlorite usually replaces amphibole and garnet as a secondary product.

Sample HSM09 (Fig. 5b), is mainly composed of amphibole (hornblend), epidote, sodic plagioclase, quartz, and calcite, with minor apatite, zircon, titanite, and garnet. Calcite mainly occurs in the samples (HSM02, 09, 10) collected from near a layer of marble intercalated concordantly or subconcordantly in host epidote-amphibolite. Clinopyroxene occasionally occurs in these samples (HSM09, 10).

Sample HSM15 (Fig. 5d), is mainly composed of amphibole (hornblend), with minor epidote, chlorite, and quartz, rutile, titanite, biotite, apatite, and opaque. Small amounts of biotite occur in some HSM series samples (HSM07, 15, 19, 20). Biotite (Fig. 7a, b, c) has never been reported before in Tonaru epidote-amphibolite samples. Only when the protoliths of amphibolite are derived from andesitic rock SiO_2 from 57 wt% to 63 wt%, or when it is a mixture of basaltic pyroclastic rock and muddy sedimentary rock, do

biotite often occur. In particular, large amount of biotites are observed in Sample HSM15.

Sample TO13 (Fig. 5c), is mainly composed of amphibole (hornblend), zosite, paragonite. Paragonite formed in the Besshi region of Sanbagawa metamorphic belt, is very hard to distinguish from muscovite under the microscope, and paragonite usually coexists with muscovite in some samples collected from the central and northern parts of the Tonaru epidote-amphibolite body. Although some lithologies of the Tonaru body contain zoisite instead of epidote or lack these epidote-group minerals, all of these are hereafter defined as epidote-amphibolite, unless otherwise stated. Epidote-amphibolites are mainly composed of amphibole, epidote/zoisite, muscovite, sodic plagioclase (Fig. 5a, b), and quartz with accessory rutile, titanite, and apatite. The TO series samples are usually poor in plagioclase and quartz, usually 0.1–10 vol%, and some samples are free of these felsic minerals (Fig. 6c). The plagioclase- and quartz-poor assemblages are also observed in the HSM series (Fig. 6d). Kyanite occurs locally in zoisite-amphibolite (e.g., Kabir *et al.*, 2016), and is usually replaced by margarite and/or a fine-grained aggregate of margarite and paragonite. Chlorite usually replaces amphibole and garnet as a secondary product. Although opaque minerals were not directly identified under reflected light microscope, most of them are probably iron sulfide minerals and ilmenite based on qualitative analyses by using an electron probe micro-analyzer (EPMA). Ilmenite grains were usually rimmed by titanite. Omphacite and its retrograde symplectitic pseudomorph were reported from the eastern (Moriyama, 1900) and entire area of the Tonaru epidote-amphibolite body (Miyagi and Takasu, 2005), respectively. However, we could not find omphacite and its pseudomorph in the epidote-amphibolite samples studied. Basic lithologies in the shear zone (samples TOCA01, 02, and TOCV)

Table 1. Mineral assemblages of Tonaru epidote-amphibolites and basic lithology in the shear zone of the Kokuryo-gawa area, Sanbagawa metamorphic belt.

Sample	Amp	Ep	Zo	Grt	Ms/Pg	Chl	Pl	Qz	Rt	Ttn
TO0801	+	+					+	+		+
TO01	+	+	+		+	s	+	+	+	+
HSM01	+	+			+	s	+	+		+
HSM02	+	+		+	+	s	+	+	+	
HSM03a	+	+			+		+	+	+	
HSM03b	+	+		+	+	s	+	+	+	
HSM004	35.3	2.1			9.3		37.9	14.6	0.6	
HSM05	+	+			+	s	+	+	+	
HSM06	+	+		+	+	s	+	+	+	
HSM07	+	+			+	s	+	+	+	
HSM08	28.3	13.8				0.8	54.1	1.4	<0.1	1.4
HSM09	15.8	56.3					0.3	18.5		1.4
HSM10	+	+			+		+	+		+
HSM11	+	+			+	s	+	+	+	+
HSM12	+	+			+	s	+	+	+	
HSM13	+	+			+		+	+		+
HSM14	+	+			+		+	+	+	+
HSM15	95.0	3.2				1.2		<0.1	0.1	0.2
HSM16	+	+			+	+		+	+	+
HSM17	+	+		+	+	s	+	+	+	+
HSM18	+	+							+	+
HSM19	+	+			+	s	+		+	+
HSM20	+	+				s			+	+
HSM21	+	+			+		+	+		+
HSM23	+	+			+		+			+
HSM24	+	+			+	s	+	+	+	+
HSM25	+	+	+		+		+	+		+
TO07	+	+	+		+	+	+	+	+	+
TO09	+	+	+		+	s	+	+	+	+
TO10	+	+	+		+	+			+	+
TO0910	40.9	<0.1	52.3		5.7		<0.1	0.9		
TO14	+	+					+	+		+
TO15	+	+	+		+	s	+	+	+	+
TO2508	+	+	+		+	+	+			+
TO16	+	+			+	+	+	+	+	+
TOCA01	37.6	7.7		12.2	0.9	<0.1	34.8	5.4	1.1	0.2
TOCA02	+	+	+	+	+	s	+	+	+	+

Table 1. Continued

Sample	Opq	Cal	Ap	Zrn	Others
TO0801			+		
TO01			+		
HSM01	+		+		
HSM02	+	+	+	+	
HSM03a			+	+	
HSM03b	+		+		
HSM004	<0.1		0.2	<0.1	
HSM05	+		+		
HSM06	+		+		
HSM07	+		+		Bt (0.1)
HSM08	0.1	7.9	<0.1	<0.1	
HSM09		+	<0.1	<0.1	Cpx
HSM10			+		
HSM11	+		+		
HSM12	+		+		
HSM13	+		+		
HSM14	+		+		
HSM15			0.1		Bt (0.1)
HSM16	+		+		
HSM17	+		+		
HSM18					Bt
HSM19	+		+		Bt
HSM20	+		+	+	
HSM21					
HSM23	+		+		
HSM24	+		+	+	
HSM25	+		+		
TO07	+		+		
TO09			+		
TO10			+		
TO0910	<0.1		<0.1	<0.1	
TO14	+		+		
TO15			+		
TO2508					
TO16	+		+		
TOCA01	<0.1		<0.1		
TOCA02	+		+		

+, primary phase; s, seondary phase. Number indicates modal composition of each mineral (vol%). Modal compositions were calculated based on analyses of 2000–2100 points.Abbreviations for minerals: Amp, amphibole; Ep, epidote; Zo, zoisite; Grt, garnet; Ms/Pg, muscovite/paragonite; Chl, chlorite; Pl, plagioclase; Qz, quartz; Rt, rutile; Ttn, titanite; Opq, opaque mineral; Cal, calcite; Ap, apatite; Zrn, zircon; Bt, biotite; Cpx, calcic clinopyroxene.

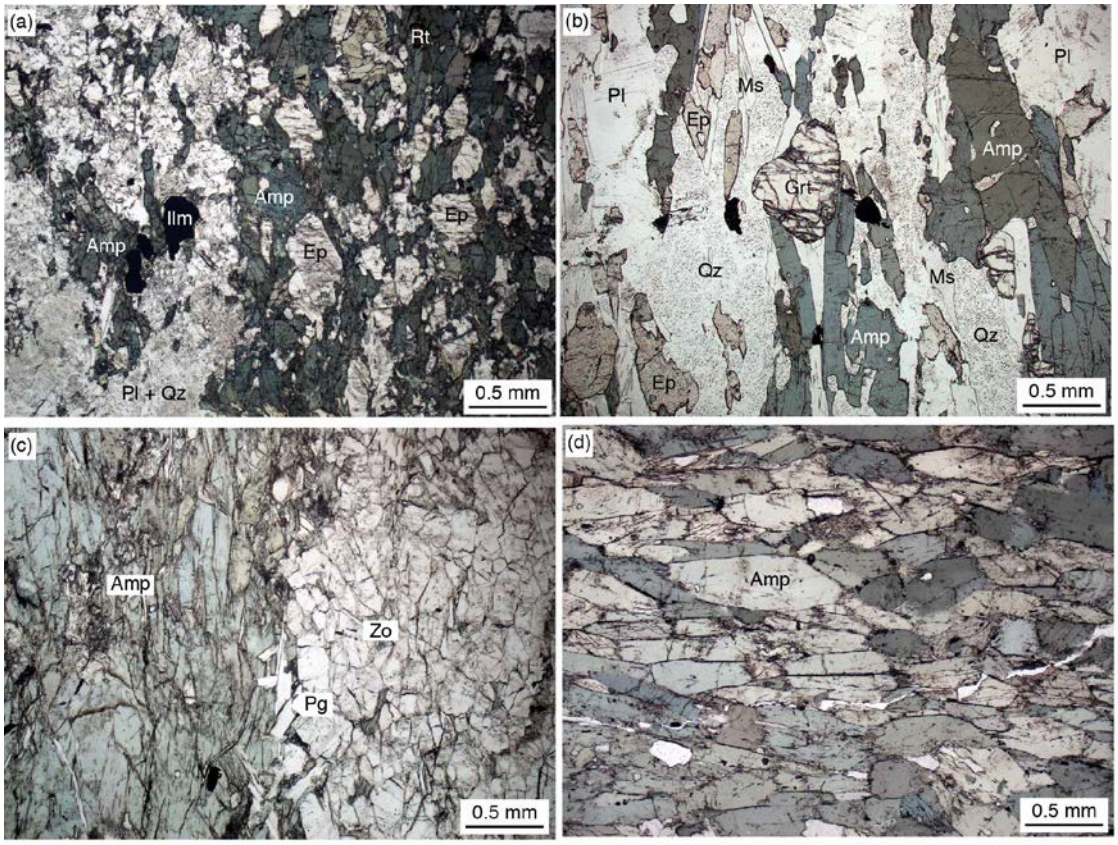

Fig. 5. Polarizing photomicrographs (plane polarized light) of the Tonaru epidote-amphibolites (a) TO10, (b) HSMS03b, (c) TO13, and (d) HSM15. Amp, amphibole; Ep, epidote; Zo, zoisite; Grt, garnet; Ms/Pg, muscovite/paragonite; Chl, chlorite; Pl, plagioclase; Qz, quartz; Rt, rutile; Ttn, titanite; Opq, opaque mineral; Cal, calcite; Ap, apatite; Zrn, zircon; Bt, biotite; Cpx, calcic clinopyroxene.

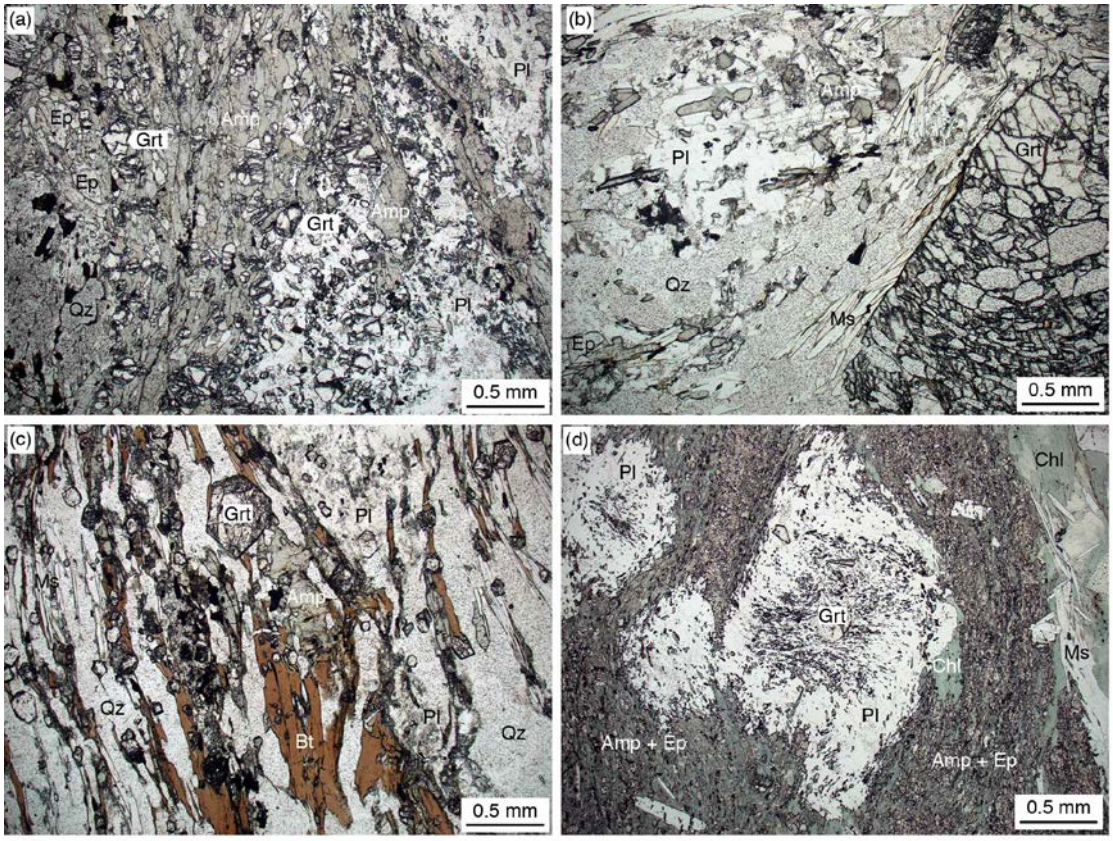

Fig. 6. Polarizing photomicrographs (plane polarized light) of (a) basic (TOCA01) and (b) pelitic (TOCP01) lithologies from the shear zone at the northern boundary between the epidote-amphibolite and pelitic schist, and (c) pelitic schist (TN02) and (d) basic schist (TN05).
Amp, amphibole; Ep, epidote; Zo, zoisite; Grt, garnet; Ms/Pg, muscovite/paragonite; Chl, chlorite; Pl, plagioclase; Qz, quartz; Rt, rutile; Ttn, titanite; Opq, opaque mineral; Cal, calcite; Ap, apatite; Zrn, zircon; Bt, biotite; Cpx, calcic clinopyroxene.

HSM19 plane

HSM19 crossed

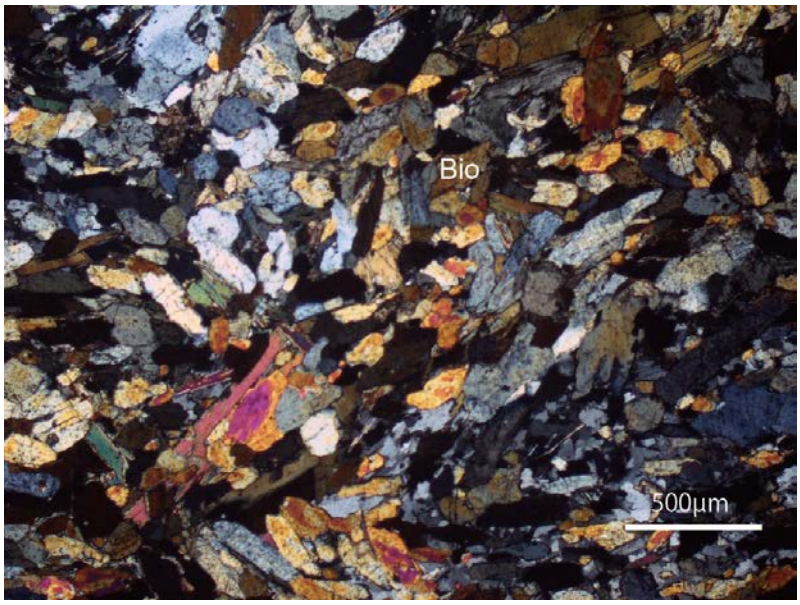

Fig. 7. Polarizing photomicrographs of biotites in the Tonaru epidote-amphibolites HSM19. Bt, biotite.

HSM02

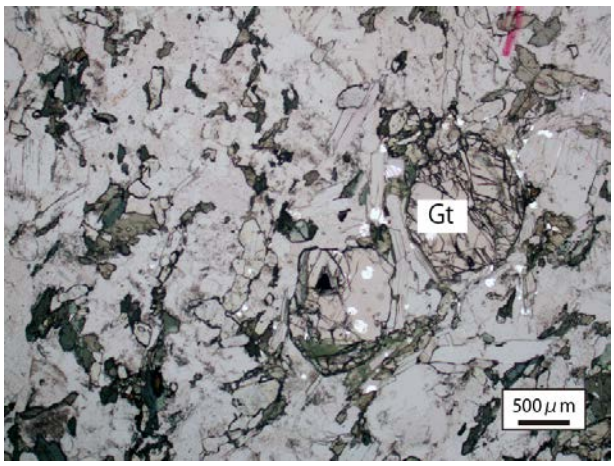

HSM03b

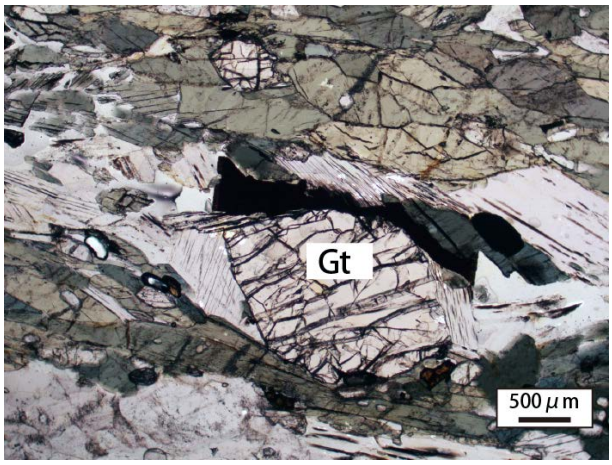

HSM06

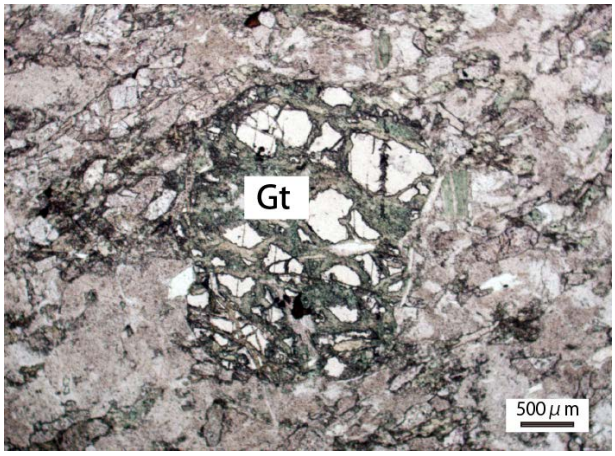

Fig. 8 Polarizing photomicrographs (plane polarized light) of garnets in the Tonaru epidote-amphibolites HSM02, HSM03b, HSM06. Gt: garnet.

consist of amphibole, epidote, sodic plagioclase, and quartz, similar to the common epidote-amphibolites in the area and basic schists of the oligoclase-biotite zone. Samples TOCA01 and 02 contain relatively fine-grained and anhedral garnet grains (Fig. 6a). Garnet grains in sample TOCV contrastingly show euhedral to subhedral form similar to those in the Sanbagawa pelitic and basic schists. Pelitic lithologies in the shear zone are generally poor in biotite and graphite and sometimes lack them (Fig. 6b). EPMA analyses confirmed that the alternating lithologies of the shear zone partly contain dolomite. Pelitic schists, which occurs on the north side of the shear zone, consist mainly of biotite, garnet, amphibole, muscovite, sodic plagioclase, and quartz, with accessory amounts of graphite, rutile, titanite, and apatite (Fig. 6c). Basic schists, which are distributed to the northern side of the pelitic schists, have mineral assemblages similar to the epidote-amphibolites, other than the absence of paragonite. However, sodic plagioclase in the basic schists usually forms porphyroblasts (Fig. 6d), in contrast to the case of epidote-amphibolite, where sodic plagioclase occurs as equigranular aggregates usually with quartz between amphibole grains (Fig. 6a, b). Thus, the basic schists are easily discriminated from the epidote-amphibolites. These pelitic and basic schists are referred to hereafter as the Tonaru pelitic and basic schists, respectively.

4. ANALYTICAL PROCEDURES

Quantitative chemical analyses of the major phases and X-ray mapping of the major phases were carried out using a JEOL JCXA-8800R (WDS + EDS) and a JXCA-733 electron-probe micro-analyzer (EPMA) from the Petrology Laboratory at the

Department of Earth and Planetary Sciences, Nagoya University. The accelerating voltage and specimen current for quantitative analyses were maintained at 15 kV and 12 nA on the Faraday cup, respectively. A beam diameter of 5 μm was used for feldspar analyses, and a diameter of 2–3 μm was used for analyzing all other phases. Well-characterized natural and synthetic phases were employed as standards. Matrix corrections were performed using the α-factor table from Kato (2005). The Fe^{3+}/Fe^{2+} values for amphibole were estimated considering the maximum value (13eCNK) proposed by Leake *et al.* (1997), while total iron was assumed as FeO for garnet. Abbreviations for minerals and end-members are after Whitney and Evans (2010).

Whole-rock compositions including Major element (Si, Al, Ca, Mg, Na, K, Ti, Fe, Mn, and P) and trace element (V, Cr, Ni, Cu, Zn, Rb, Sr, Y, Zr, Mb, and Ba) compositions were determined by X-ray fluorescence spectrometry (XRF) using a Shimadzu XRF-1800 from the Chronological Laboratory at the Institute for Space-Earth Environmental Research (ISEE), Nagoya University, and Rigaku ZSX Primus II with rhodium target X-ray tubes from the Petrology Laboratory at the Department of Earth and Planetary Sciences, Nagoya University, operating at 40 kV/70 mA and 60 kV/50 mA, respectively. Detailed XRF analytical procedures are described in Sugisaki *et al.* (1977; 1981) and Nakazaki *et al.* (2004). The glass beads for major and trace element analyses were prepared by fusing mixtures of powdered samples and lithium borate in the following weight ratios: 0.7: 6.0 (major) and 2.0: 3.0 (trace) for the Shimadzu XRF-1800, and 0.5: 5.0 (major) and 1.5: 6.0 (trace) for the Rigaku ZSX Primus II. Reference samples of sedimentary and igneous rocks provided by the Geological Survey of Japan (GSJ) and composite standards prepared by Morishita and Suzuki (1993) and Yamamoto and Morishita (1997) were used for calibrations. The major and

Supplementary Table S01. Average compositions of amphibole from the Tonaru epidote-amphibolites and basic lithology in the shear zone of the Kokuryo-gawa area, Sanbagawa metamorphic belt.

Sample	TO01	ME1806T†	KK1805†	DA2504†	TO07
	P	P	P	P	S
wt%					
SiO_2	46.08	43.07	44.23	42.89	54.61
TiO_2	0.29	0.57	0.53	0.52	0.02
Al_2O_3	13.63	15.77	12.28	14.92	1.80
FeO*	8.82	14.78	15.12	14.53	11.38
MnO	0.19	0.30	0.27	0.33	0.26
MgO	13.66	10.43	10.88	10.03	16.08
CaO	11.12	10.51	10.48	10.06	12.05
Na_2O	1.97	2.85	2.56	2.87	0.65
K_2O	0.26	0.46	0.83	0.39	0.08
Total	96.02	98.74	97.18	96.54	96.93
Formulae (O = 23)					
Si	6.637	6.204	6.520	6.318	7.849
Ti	0.031	0.062	0.059	0.058	0.002
A	2.314	2.677	2.133	2.590	0.305
Fe^{3+}**	0.320	0.666	0.512	0.589	0.086
Fe^{2+}**	0.743	1.115	1.352	1.201	1.282
Mn	0.023	0.037	0.034	0.041	0.032
Mg	2.932	2.239	2.390	2.202	3.445
Ca	1.716	1.622	1.655	1.588	1.856
Na	0.550	0.796	0.732	0.820	0.181
K	0.048	0.085	0.156	0.073	0.015
Total	15.314	15.503	15.543	15.480	15.053

* Total iron as FeO.
** Calculated values. See text.
† Samples ME1806T, KK1805, and DA2504 were collected from the same outcrops of sample HSM03a, b, HSM09, and HSM25, respectively.
Abbrebiations are: P, primary phase; S, secondary phase.

Supplementary Table S01. Continued

TO09	TO0910	TO14	TO15	TO16	TOCA01
P	P	P	P	P	P
54.08	46.45	54.39	48.24	42.98	43.06
0.04	0.17	0.14	0.17	0.42	0.50
3.84	14.16	6.60	11.33	15.33	15.11
5.76	6.65	5.47	7.11	12.39	13.08
0.14	0.12	0.18	0.16	0.24	0.10
19.24	14.78	17.66	16.00	11.04	10.56
12.73	11.05	11.79	11.81	10.47	11.07
0.94	2.39	1.01	1.92	2.75	2.27
0.18	0.40	0.46	0.14	0.52	0.51
96.95	96.17	97.70	96.88	96.14	96.26
7.618	6.639	7.554	6.842	6.322	6.361
0.004	0.018	0.015	0.018	0.046	0.056
0.637	2.385	1.080	1.894	2.657	2.631
0.000	0.182	0.000	0.242	0.424	0.287
0.679	0.613	0.635	0.602	1.100	1.329
0.017	0.015	0.021	0.019	0.030	0.013
4.039	3.149	3.656	3.383	2.420	2.325
1.921	1.692	1.754	1.795	1.650	1.752
0.257	0.662	0.272	0.528	0.784	0.650
0.032	0.073	0.081	0.025	0.098	0.096
15.204	15.428	15.068	15.348	15.531	15.500

* Total iron as FeO.
** Calculated values. See text.
† Samples ME1806T, KK1805, and DA2504 were collected from the same outcrops of sample HSM03a, b, HSM09, and HSM25, respectively.
Abbrebiations are: P, primary phase; S, secondary phase.

Supplementary Table S2. Major and trace element compositions of Tonaru epidote-amphibolites from the Kokuryo-gawa area, Sanbagawa metamorphic belt.

Sample	TO0801	TO01	HSM01	HSM02	HSM03A	HSM03B	HSM04	HSM05	HSM06
XRF	SH	SH	SH	SH	SH	SH	SH	SH	SH
(wt%)									
SiO_2	45.07	41.42	54.31	54.37	54.95	51.68	61.78	61.98	60.41
TiO_2	0.70	0.95	0.66	0.69	0.74	1.14	0.71	0.68	0.57
Al_2O_3	16.07	19.08	18.29	19.03	16.39	17.15	16.24	19.47	17.14
Fe_2O_3*	11.08	14.90	7.62	8.45	8.32	11.08	6.35	4.74	5.95
MnO	0.17	0.24	0.11	0.18	0.14	0.22	0.10	0.08	0.12
MgO	6.37	9.20	2.92	2.83	5.34	6.35	5.26	2.10	2.04
CaO	16.64	11.22	8.93	6.73	6.96	7.64	5.93	4.65	5.36
Na_2O	1.31	1.27	5.14	4.71	3.88	2.98	4.20	6.37	4.59
K_2O	0.07	0.52	0.17	0.61	0.92	1.43	1.10	0.75	0.81
P_2O_5	0.18	0.24	0.21	0.26	0.23	0.26	0.18	0.28	0.19
LOI**									
Total	97.66	99.04	98.36	97.86	97.87	99.93	101.85	101.10	97.18
(ppm)									
V	263	253	137	130	158	217	112	79	71
Cr	24	16	7	8	52	29	43	25	12
Co	51	54	35	35	39	48	27	20	10
Ni	5	20	2	2	27	12	19	16	11
Cu	240	151	28	0	14	45	0	23	0
Zn	69	178	82	95	59	82	58	61	48
Ga									
Rb	12	17	12	20	18	21	22	19	17
Sr	511	702	725	787	404	252	392	1065	513
Y	11	23	14	19	23	31	16	6	16
Zr	33	59	64	103	108	106	150	83	78
Nb									
Ba	9	220	55	189	340	570	372	420	228
As	58	51	48	53	52	52	48	51	36
Pb	9	8	9	5	6	5	4	7	8
Th	0	5	0	0	1	0	0	0	3

*Total iron as Fe2O3.
** loss on ignition.
Abbreviations are: SH, SHIMADZU XRF-1800; RG, Rigaku ZSX Primus II.

Supplementary Table S2. (continued)

Sample No.	HSM07	HSM08	HSM09	HSM10	HSM11	HSM12	HSM13	HSM14	HSM15
XRF	SH	SH	SH	SH	SH	SH	SH	SH	SH
(wt%)									
SiO_2	59.23	53.20	51.18	49.23	48.23	57.53	54.54	56.10	48.49
TiO_2	0.70	0.80	0.72	0.50	0.92	0.69	0.85	0.70	1.33
Al_2O_3	19.07	18.71	15.86	18.92	19.11	19.27	16.43	17.39	9.14
Fe_2O_3*	5.67	8.35	7.47	5.81	11.36	6.25	7.59	7.04	14.73
MnO	0.09	0.15	0.11	0.14	0.18	0.11	0.13	0.10	0.20
MgO	2.59	3.01	3.94	2.51	4.68	2.45	4.16	4.16	13.04
CaO	6.39	8.18	18.60	16.92	10.52	7.05	10.90	8.65	9.64
Na_2O	6.17	6.01	0.38	3.60	4.00	5.21	3.65	5.09	2.05
K_2O	0.43	0.40	0.11	0.05	0.28	0.63	0.34	0.41	0.40
P_2O_5	0.26	0.25	0.31	0.47	0.32	0.32	0.25	0.24	0.06
LOI**				2.55					0.88
Total	100.60	99.06	98.68	100.70	99.60	99.51	98.84	99.88	99.96
(ppm)									
V	111	144	131	116	215	101	127	124	241
Cr	22	10	23	22	38	26	38	18	1037
Co	21	36	27	17	47	27	32	33	304
Ni	14	1	9	5	12	12	16	7	460
Cu	3	48	0	6	23	24	28	16	38
Zn	53	80	85	33	118	53	65	61	141
Ga									
Rb	13	13	11	11	12	17	13	15	10
Sr	976	719	964	1047	845	1035	655	673	26
Y	13	20	18	12	22	15	24	21	18
Zr	69	68	80	67	53	167	135	95	210
Nb									
Ba	226	200	36	21	73	265	136	123	104
As	46	53	50	42	48	45	44	48	50
Pb	8	5	9	11	5	7	8	7	2
Th	0	0	2	2	0	0	2	3	10

Supplementary Table S2 (continued)

Sample No.	HSM16	HSM17	HSM18	HSM19	HSM20	HSM21	HSM23	HSM24	HSM25
XRF	SH	SH	SH	SH	SH	SH	SH	SH	SH
(wt%)									
SiO_2	45.43	48.21	47.71	46.64	48.65	53.76	49.23	51.41	46.32
TiO_2	0.87	0.85	1.07	0.88	0.41	0.11	0.88	0.92	0.51
Al_2O_3	20.02	17.75	9.93	19.87	8.05	20.55	13.85	16.68	20.83
Fe_2O_3*	11.83	10.99	10.50	9.80	10.44	4.85	9.66	8.93	9.63
MnO	0.18	0.17	0.14	0.15	0.15	0.08	0.14	0.15	0.15
MgO	5.33	5.72	14.88	4.70	15.87	4.75	10.52	5.22	6.12
CaO	11.01	11.12	11.53	11.87	11.47	10.27	12.90	10.01	12.75
Na_2O	3.14	2.84	1.91	3.33	1.64	3.87	1.75	4.00	2.40
K_2O	0.34	0.31	0.69	0.67	0.54	0.79	0.63	0.71	0.64
P_2O_5	0.22	0.18	0.04	0.21	0.20	0.03	0.33	0.25	0.11
LOI**					2.94				
Total	98.37	98.14	98.40	98.12	100.36	99.06	99.89	98.28	99.46
(ppm)									
V	272	259	275	204	212	67	195	211	227
Cr	46	62	347	27	1291	60	506	94	150
Co	54	52	72	43	55	7	52	43	45
Ni	10	26	108	9	397	32	163	34	39
Cu	46	23	16	105	1	11	15	60	20
Zn	92	94	89	72	91	20	129	87	85
Ga									
Rb	15	14	16	23	10	20	20	19	18
Sr	656	610	108	1277	111	369	800	673	717
Y	22	19	10	19	9	3	11	21	8
Zr	71	82	53	44	114	20	86	83	25
Nb									
Ba	152	42	52	528	49	66	91	241	120
As	51	46	51	43	47	38	47	43	51
Pb	5	8	6	9	4	8	5	10	6
Th	1	2	4	3	8	4	9	8	0

Supplementary Table S2 (continued)

Sample No.	TO07	TO09	TO10	TO0910	TO14	TO15	TO2508	TO16
XRF	SH	RG	SH	RG	SH	RG	RG	SH
(wt%)								
SiO_2	44.89	46.51	43.07	47.24	47.93	44.74	44.81	49.76
TiO_2	0.17	0.26	0.15	0.14	0.16	0.10	0.09	0.91
Al_2O_3	22.78	18.66	17.78	20.54	14.02	16.39	20.68	18.28
Fe_2O_3*	6.10	5.16	7.64	4.90	6.79	6.07	5.12	10.24
MnO	0.11	0.08	0.11	0.07	0.12	0.12	0.06	0.17
MgO	8.19	7.17	13.00	7.79	11.76	10.53	9.31	4.59
CaO	14.22	18.07	11.66	14.11	16.86	16.78	16.51	9.16
Na_2O	1.99	1.12	1.39	2.59	0.61	0.60	0.94	4.70
K_2O	0.16	0.24	0.91	0.33	0.07	0.07	0.06	0.33
P_2O_5	0.03	0.01	0.02	0.02	0.01	0.01	0.02	0.26
LOI**		1.81	3.40	1.85		2.65	2.81	
Total	98.64	99.09	99.13	99.58	98.33	98.06	100.41	98.40
(ppm)								
V	93		65		212			144
Cr	292	7	373	231	48	439	361	295
Co	23	18	55	47	44	44	36	40
Ni	84	5	150	68	11	142	90	85
Cu	0	14	0	65	16	12	4	13
Zn	40	20	46	37	106	36	34	30
Ga		8		9		10	8	
Rb	14	4	28	5	13	0	0	12
Sr	557	481	585	572	603	551	735	363
Y	4	5	5	3	23	5	3	5
Zr	22	8	27	5	87	4	3	24
Nb		0		0		0	0	
Ba	8	89	111	91	85	71	70	19
As	44		50		48			53
Pb	5	0	4	6	7	0	1	4
Th	0	8	1	6	1	3	6	0

Supplementary Table S3. Major and trace element compositions of basic and pelitic lithologies from the shear zone of the Kokuryo-gawa area, Sanbagawa metamorphic belt.

Sample No.	TOCA01	TOCA02	TOCV	TOCP01
XRF	SH	SH	SH	SH
(wt%)				
SiO_2	52.62	47.57	53.94	66.58
TiO_2	0.89	0.90	2.23	0.70
Al_2O_3	17.93	17.00	13.52	15.12
Fe_2O_3*	9.79	12.10	13.81	5.34
MnO	0.19	0.19	0.22	0.12
MgO	4.54	6.81	5.12	2.92
CaO	7.93	9.77	7.32	2.92
Na_2O	3.87	2.77	1.88	1.86
K_2O	0.91	0.79	0.47	2.35
P_2O_5	0.19	0.24	0.21	0.14
LOI**				
Total	98.86	98.14	98.72	98.05
(ppm)				
V	191	262	354	101
Cr	48	67	131	117
Co	39	57	69	23
Ni	9	31	41	63
Cu	63	75	28	35
Zn	72	105	142	60
Ga				
Rb	27	26	17	69
Sr	656	497	58	249
Y	18	18	45	25
Zr	140	85	124	162
Nb				
Ba	150	125	55	649
As	54	51	48	48
Pb	16	12	9	11
Th	0	1	0	11

* Total iron as Fe_2O_3.

** loss on ignition.

Abbreviations are: Blt, basic lithologye; Plt, pelitic lithology; SH, SHIMADZU XRF-1800.

Supplementary Table S4. Major and trace element compositions of pelitic schists from the Kokuryo-gawa area, Sanbagawa metamorphic belt.

Sample No.	TN01	TN2401b	TN0907	TN0906	TN02	TN2404	TN0904	TN0902
XRF	RG	RG	RG	RG	RG	RG	RG	RG
(wt%)								
SiO_2	63.80	63.41	63.22	67.11	63.25	65.02	68.75	71.02
TiO_2	0.80	0.93	0.77	0.59	0.96	0.66	0.58	0.51
Al_2O_3	16.23	14.99	14.08	14.17	14.26	16.52	15.68	14.67
Fe_2O_3*	7.40	7.32	6.15	5.21	8.25	6.61	4.71	4.11
MnO	0.36	0.27	0.19	0.14	0.36	0.27	0.08	0.07
MgO	2.84	3.47	4.96	4.07	3.31	2.32	1.51	1.36
CaO	1.84	2.45	3.76	2.27	3.03	1.16	0.58	0.76
Na_2O	1.93	2.09	2.64	3.20	2.64	1.78	2.91	2.64
K_2O	3.07	2.46	1.77	1.49	1.85	3.19	2.86	3.16
P_2O_5	0.11	0.19	0.15	0.11	0.13	0.10	0.08	0.08
LOI**	2.70	2.21			2.43	2.93		
Total	101.08	99.79	97.69	98.36	100.47	100.56	97.74	98.38
(ppm)								
V								
Cr	72	105	280	187	101	68	63	54
Co	21	24	23	20	26	19	13	8
Ni	47	70	146	105	55	46	36	21
Cu	74	84	68	74	81	54	49	32
Zn	107	105	74	66	100	121	91	74
Ga	21	20	13	17	17	21	19	18
Rb	125	95	66	63	82	154	105	131
Sr	159	220	310	293	195	165	150	149
Y	28	23	23	21	30	21	27	24
Zr	151	144	137	146	138	150	165	156
Nb	14	16	11	10	11	14	13	12
Ba	540	398	211	257	343	409	505	516
As								
Pb	18	21	16	15	16	23	27	22
Th	14	16	12	13	13	15	15	16

* Total iron as Fe_2O_3.

** loss on ignition.
Abbreviations are: RG, Rigaku ZSX Primus II.

Supplementary Table S5. Major and trace element compositions of basic schists from the Kokuryo-gawa area, Sanbagawa metamorphic belt.

Sample No.	TN0905	TN03	TN04	TN05	TN0903	TN0901
XRF	RG	RG	RG	RG	RG	RG
(wt%)						
SiO_2	48.95	53.69	44.55	45.00	47.57	47.64
TiO_2	0.79	0.93	0.98	1.44	1.01	1.56
Al_2O_3	18.34	14.94	18.13	16.77	18.54	16.18
Fe_2O_3*	11.12	8.73	11.13	12.47	10.02	11.59
MnO	0.19	0.24	0.17	0.25	0.14	0.22
MgO	4.79	9.60	4.37	5.20	3.20	6.16
CaO	8.91	6.09	10.56	12.14	13.22	10.11
Na_2O	4.15	5.35	3.40	2.61	3.03	2.94
K_2O	0.35	0.31	1.08	0.62	0.40	0.42
P_2O_5	0.17	0.07	0.07	0.13	0.12	0.19
LOI**		1.73	3.84	3.10	2.80	2.27
Total	97.76	101.68	98.28	99.73	100.05	99.28
(ppm)						
V						
Cr	14	542	504	463	446	200
Co	29	37	58	61	37	44
Ni	6	154	164	163	107	69
Cu	54	31	35	37	31	188
Zn	98	127	128	127	72	83
Ga	19	17	15	16	13	15
Rb	4	5	19	19	5	10
Sr	700	90	199	197	200	249
Y	13	21	21	20	30	29
Zr	28	76	68	63	62	112
Nb	0	5	4	3	6	12
Ba	43	52	48	42	74	125
As						
Pb	7	0	0	0	1	0
Th	4	9	9	6	10	8

* Total iron as Fe_2O_3.
** loss on ignition.
Abbreviations are: RG, Rigaku ZSX Primus II.

trace element compositions of epidote-amphibolite, pelitic schist, and basic schist are listed in Supplementary Tables S2–S5.

For REE (La, Ce, Pr, Nd, Pm, Sm, Eu, Gd, Tb, Dy, Er, Tm, Yb and Lu) analyses, whole-rock powder samples were digested using the alkali fusion method with lithium tetraborate as a flux. After dissolution in HCl, the REEs were separated using cation exchange resin. The REE concentrations were measured with an Agilent 7500 inductively-coupled plasma mass spectrometer at Kwansei Gakuin University. Indium was used as an internal standard. The REE compositions of the epidote-amphibolites and pelitic schists are listed in Supplementary Table S6.

5. MINERALOGY

5.1 Amphibole

Amphibole grains in the Tonaru body are usually homogeneous or have weak prograde zoning with increasing Al content from the crystal center toward the mantle. These primary phases are replaced by retrograde actinolite along fractures and cleavages and around grain margins. In some cases, primary amphibole grains were completely replaced by aggregates of fine-grained actinolite. The average compositions of amphiboles from some representative Tonaru epidote-amphibolites are listed in Supplementary Table S1. Primary amphibole grains have variable compositions with Si = 7.8–6.0 atoms per formula unit (apfu) for O = 23, $^{[A]}(Na + K)$ = 0.1–0.7 apfu, and X_{Mg}

value [= Mg/(Mg + Fe^{2+})] = 0.56–0.94 (Fig. 9), where $^{[A]}$(Na + K) indicates alkaline contents in the largest and variably coordinated A-site. These amphiboles mostly belong to magnesiohornblende–tschermakite/pargasite, according to the nomenclature of Leake *et al.* (1997). The primary amphibole compositions in samples collected from the marginal part of the Tonaru body, however, tend to be more enriched in ferrotschermakitic/ferropargasitic (lower Si and X_{Mg} contents) components than those collected from the interior of the body (Fig. 10). Plagioclase grains are sodic with average $An_{10–20}$ compositions (Enami, 1982). Although garnet grains in some Tonaru epidote-amphibolites show concentric growth zoning (Supplementary Fig. S3a, b) similar to cases in other Sanbagawa metamorphic rocks, those in most samples in this study display irregular heterogeneity in their compositions (Supplementary Fig. S3). Both types of garnet grains are rimed and replaced along cracks by distinct spessartine-rich garnet to a varying degree as reported by Matsuura *et al.* (2013), and consequently show relatively wide compositional ranges of $Alm_{50–65}Sps_{1–13}Prp_{9–22}Grs_{15–33}$. The compositionally heterogeneous core probably represents formation during the prograde eclogite facies stage prograde eclogite facies stage and subsequent resorption during the exhumation and hydration stage, as proposed for most samples from the eclogite unit (Kouketsu *et al.*, 2014; Enami *et al.*, 2017). This suggests that epidote-amphibolites including these garnet-bearing samples belong to the eclogite unit as advocated by Moriyama (1990) and Miyagi and Takasu (2005). The spessartine compositions around the heterogeneous core and along the cracks probably represent recrystallization during the subsequent prograde epidote-amphibolite facies stage. Coexisting zoisite and epidote have Y_{Fe} [= Fe^{3+}/(Fe^{3+} + Al)] values of 0.039 ± 0.005 and 0.127 ± 0.011, respectively, suggesting a miscibility gap between the two phases (Enami

and Banno, 1980). On the other hand, zoisite and epidote, which do not coexist with each other, have lower and higher Y_{Fe} values of 0.01–0.03 and 0.16–0.21, respectively, than those of the coexisting phases.

Supplementary Table S6. Rare earth element abundances of Tonaru epidote-amphibolites and basic and pelitic lithologies from the shear zone of the Kokuryo-gawa area, Sanbagawa metamorphic belt.

	Tonaru body						Shear zone	
	Epidote-amphibolite						Bsl	Pel
	HSM05	HSM12	HSM15	HSM20	TO07	TO10	TOCV	TOCP01
La	14.26	16.42	48.28	16.66	1.65	2.71	7.13	29.34
Ce	28.07	33.20	119.28	33.70	3.88	5.61	19.36	61.33
Pr	3.50	4.17	14.21	4.03	0.55	0.77	3.22	6.88
Nd	14.99	17.89	62.62	16.04	2.63	3.53	16.78	25.94
Sm	2.89	3.65	13.60	3.27	0.67	0.97	5.50	5.16
Eu	1.32	1.48	2.49	0.81	0.31	0.33	1.85	1.18
Gd	2.48	3.44	10.16	2.82	0.72	0.99	7.06	4.73
Tb	0.29	0.48	1.13	0.36	0.11	0.16	1.28	0.70
Dy	1.46	2.79	4.82	1.85	0.72	0.91	8.60	4.14
Ho	0.26	0.55	0.74	0.33	0.15	0.18	1.85	0.82
Er	0.70	1.55	1.82	0.84	0.44	0.46	5.41	2.43
Tm	0.09	0.21	0.23	0.10	0.07	0.06	0.78	0.35
Yb	0.57	1.35	1.52	0.64	0.44	0.35	5.16	2.32
Lu	0.09	0.21	0.22	0.10	0.07	0.05	0.77	0.35
Y	6.83	14.27	16.22	8.18	3.80	4.09	46.53	21.85

Abbreviations are: Bsl basic lens; Pel, pelitic lens.

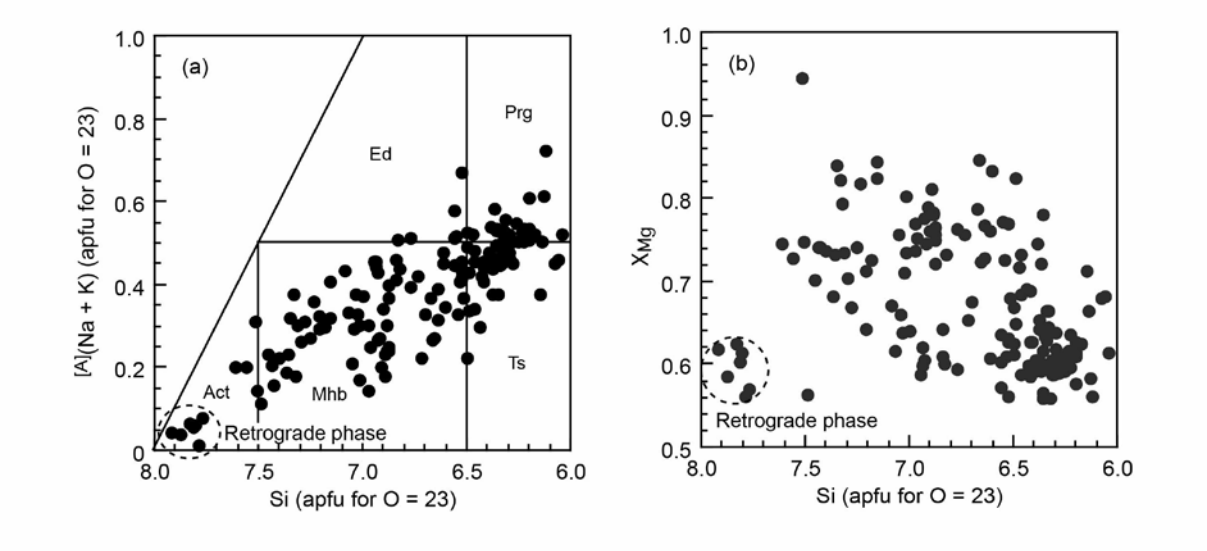

Fig. 9. Amphibole compositional variations of the Tonaru epidote-amphibolites, (a) Si-[A](Na + K) and Si-XMg diagrams (Enami, unpublished data). Abbreviations for minerals are: Act, actinolite; Ed, edenite; Mhb, Magnesio-hornblende; Prg, pargasite; Ts, tschermakite.trace elements (Cr, Ni, Sr, and Ba) of the same samples shown in Fig. 6. The average compositions of the Iratsu (IR) and Seba (SB) epidote-amphibolites and other Sanbagawa basic and pelitic schists reported in the literature are also shown in the rightmost columns of these figures for comparison.

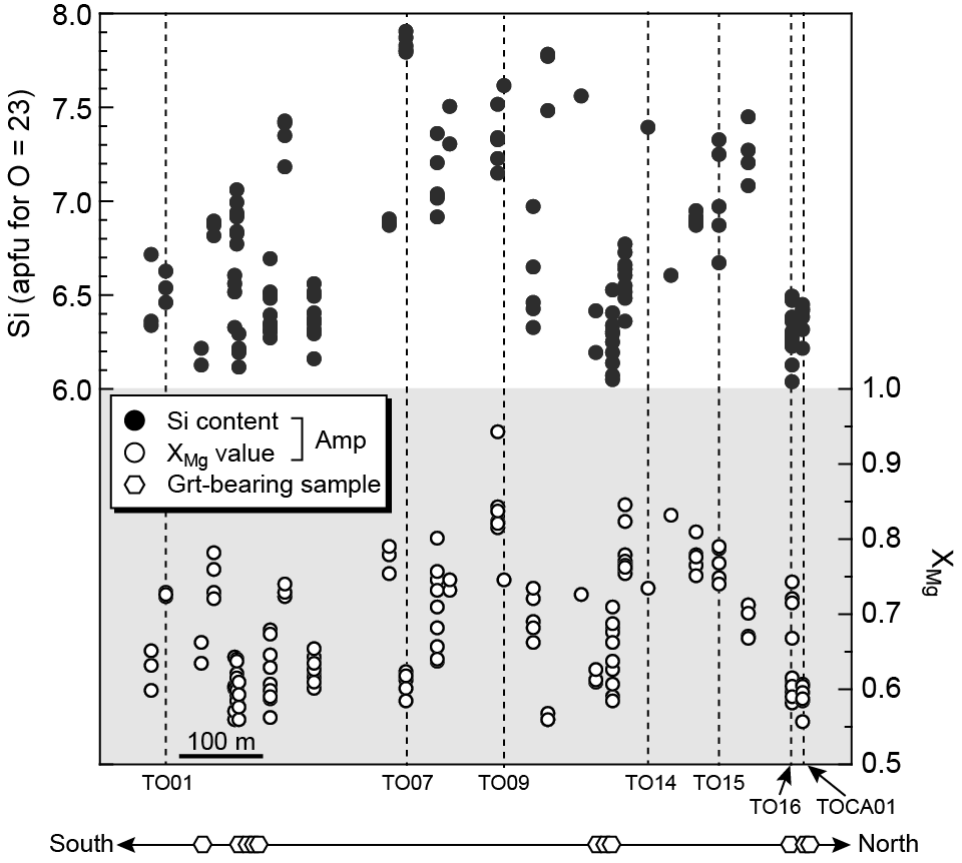

Fig. 10. Compositional variations of amphibole and occurrences of garnet in the Tonaru epidote-amphibolites along the Kokuryo River route (Enami, unpublished data).

5.2 Garnet

The garnet grain from the shear zone Sample HSM29, which located in Northern margin of intercalated within the epidote-amphibolites at the southern part of the Tonaru body. The pelitic rocks contain composite zoned garnet with paragonite inclusions (Fig. 11), and this kind of garnet is divided into inner and outer segments because of the compositional changes in Mn content, and paragonite inclusions occur in the inner segment. In the inner segment, the Mn content decreases towards the rim, increases at the boundary between the inner and outer segments, and then decreases again in the outer segment towards the outermost rim. The Ca content increases towards the boundary between the inner and outer segments slowly , and increases at the boundary, decreases at the outer segment. The Mg content increase at the boundary between the inner and outer segments.The Fe content shows a monotonic increase from the core to mantle in the inner segments, and then slightly decreases towards the outermost rim (Fig. 12).

6. WHOLE-ROCK CHEMISTRY

6.1. Systematic variations in major and trace elements along the Kokuryo River

Figures 11 and 12 show variations of selected major and trace elements, respectively, in the Tonaru epidote-amphibolite and basic and pelitic schists along the Kokuryo River.

The average compositions of the Iratsu and Seba epidote-amphibolites, and Sanbagawa common basic and pelitic schists are also shown in the rightmost columns of these figures for comparison. Data sources are listed in the captions of each figures.

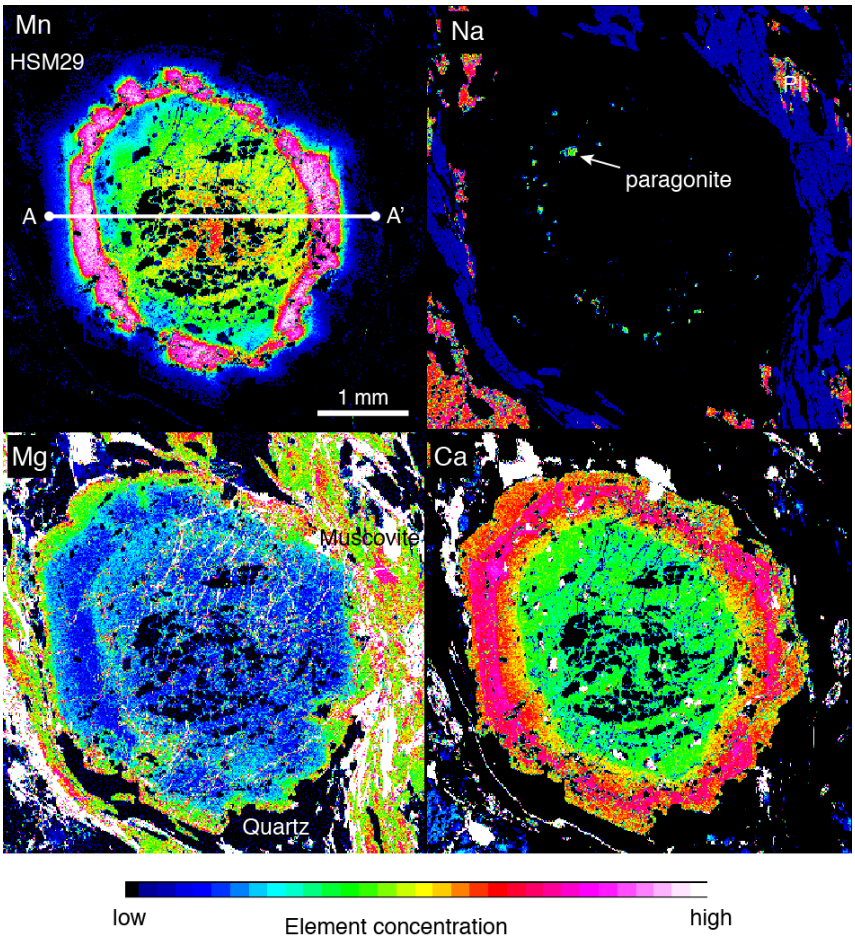

Fig. 11. X-ray mapping images of a garnet porphyroblast (Sample HSM29).

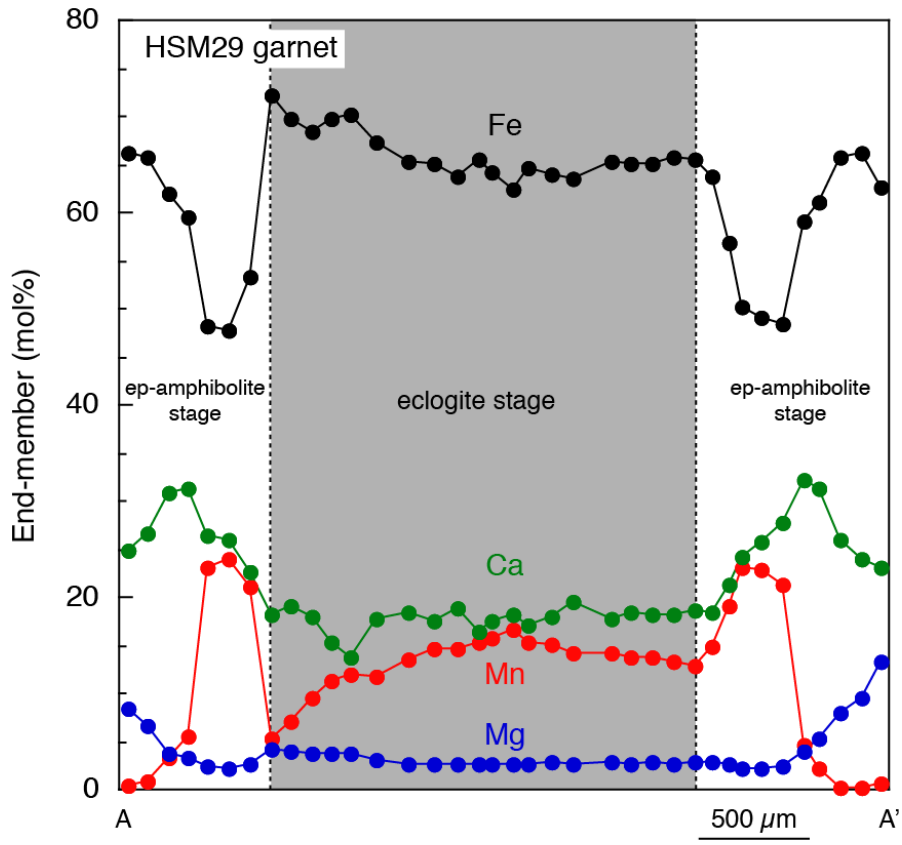

Fig. 12. Compositional profile of garnet porphyroblast in HSM29 along the white line A–A' traced in Fig. 11.

6.1.1. Epidote-amphibolite

The epidote-amphibolites have variable major elements: SiO_2 = 41.4–62.0 wt%, Al_2O_3 = 8.1–23.2 wt%, FeO* = 4.3–13.4 wt%, MgO = 2.0–15.9 wt%, CaO = 4.7–18.6 constant, SiO_2-poor concentrations (43.1–47.9 wt%), low FeO*/MgO (0.50–0.67), and high X_{CaO} (0.83–0.96) compositions (Fig. 11a, c, d). These chemical characteristics are similar to the Iratsu and Seba epidote-amphibolites with SiO_2 = 47.3 ± 0.3 wt% and X_{CaO} = 0.82 ± 0.11, although the Iratsu and Seba epidote-amphibolites contain relatively higher FeO*/MgO values (1.6 ± 0.8). The three samples collected near the southern andnorthern margins of the Tonaru body (TO0801, TO01, and TO16) also have similar SiO_2 (41.4–49.8 wt%) and X_{CaO} (0.65–0.92) contents as the typical epidote-amphibolites, which exhibit a metamorphosed layered gabbro texture, of the Tonaru, Iratsu, and Seba bodies. The FeO*/MgO (1.46–2.01) values of the latter three samples are similar to those of the Iratsu and Seba epidote-amphibolites and are higher than those of the aforementioned seven samples (TO07–TO2508) from the middle to northern regions of the Tonaru body. In contrast, epidote-amphibolite samples collected from an 80–90 m wide zone near the southern boundary (HSM series) exhibit quite variable chemical compositions (Fig. 11a, c, d), as seen for SiO_2 (45.4–62.0 wt%), Al_2O_3 (8.0–20.8 wt%), FeO*/MgO (0.6–2.7), and lower X_{CaO} [= CaO/(CaO + Na_2O + K_2O)] (0.40–0.97). whole-rock compositions, although the controlling factors cannot be

well understood in this study. Trace elements show compositional trends similar to major elements

(Fig. 12). The seven samples from TO07 to TO2508, which are almost certainly layered metagabbro, have Cr (7–439 ppm), Ni (5–150 ppm), Sr (481–735 ppm), and Ba (8–111 ppm).

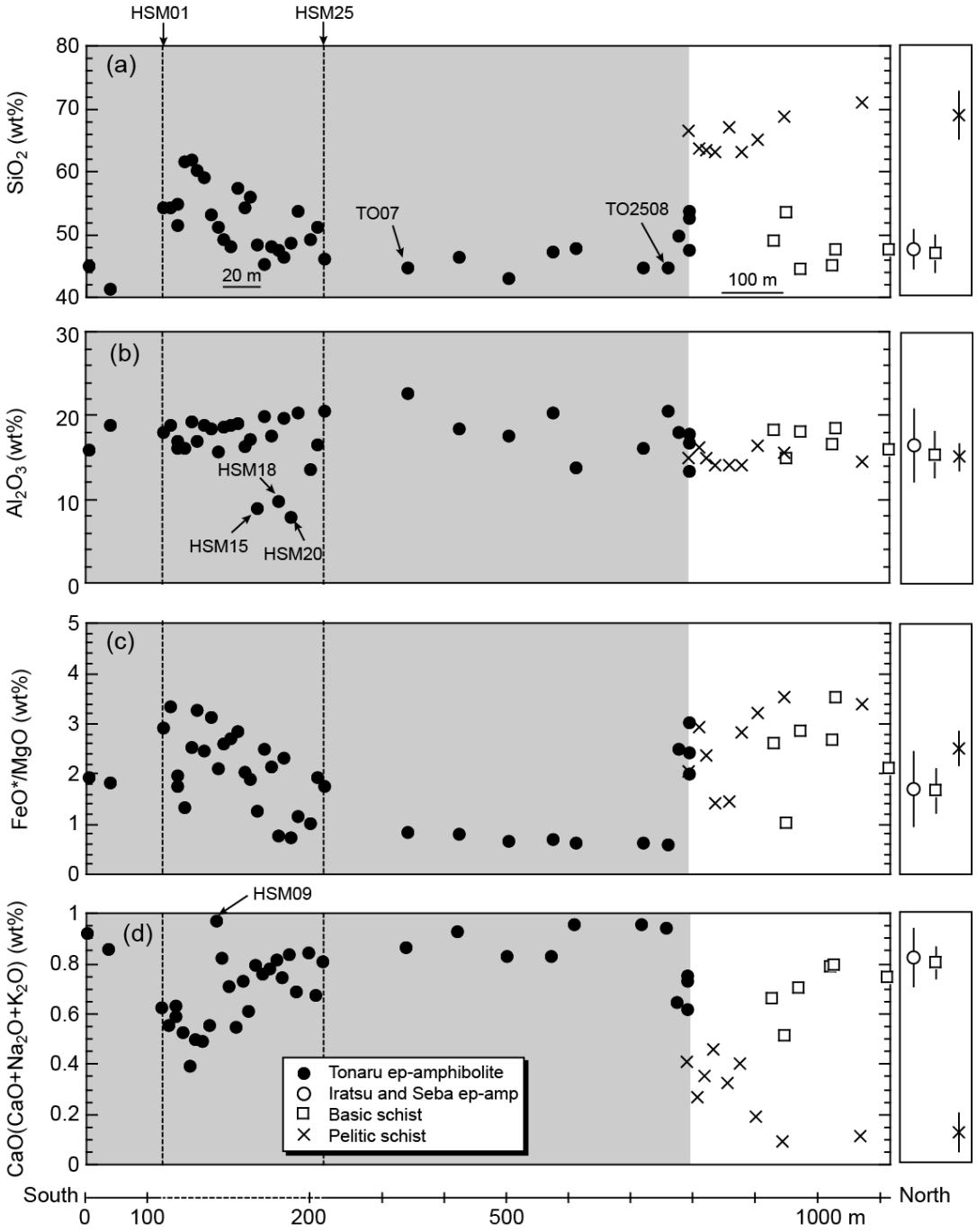

Fig. 11. Variations (wt%) of (a) SiO_2 and (b) Al_2O_3 concentrations, and (c) FeO*/MgO and (d) CaO/(CaO + Na_2O + K_2O) values of the Tonaru epidote-amphibolites along the Kokuryo River FeO* indicates total iron as FeO. Data sources are: Tonaru epidote-amphibolites (this study), Iratsu and Seba epidote-amphibolites (Goto and Banno, 1990; Aoya *et al*., 2006; Utsunomiya *et al*., 2011; Endo *et al*., 2012; Weller *et al*., 2015; Enami, unpublished data), basic schists (Banno, 1964; Ernst *et al*., 1970; Okamoto *et al*., 2000; Nozaki *et al*., 2006; Utsunomiya *et al*., 2011; Enami, unpublished data), and pelitic schists (Banno, 1964; Ernst *et al*., 1970; Goto *et al*., 1996; Kiminami and Ishihama, 2003; Zaw Win Ko *et al*., 2005; Aoya *et al*., 2006; Kiminami, 2010; Fujiwara *et al*., 2011; Utsunomiya *et al*., 2011; Enami, unpublished data). Some data for basic schists with SiO_2 < 40wt% were omitted.

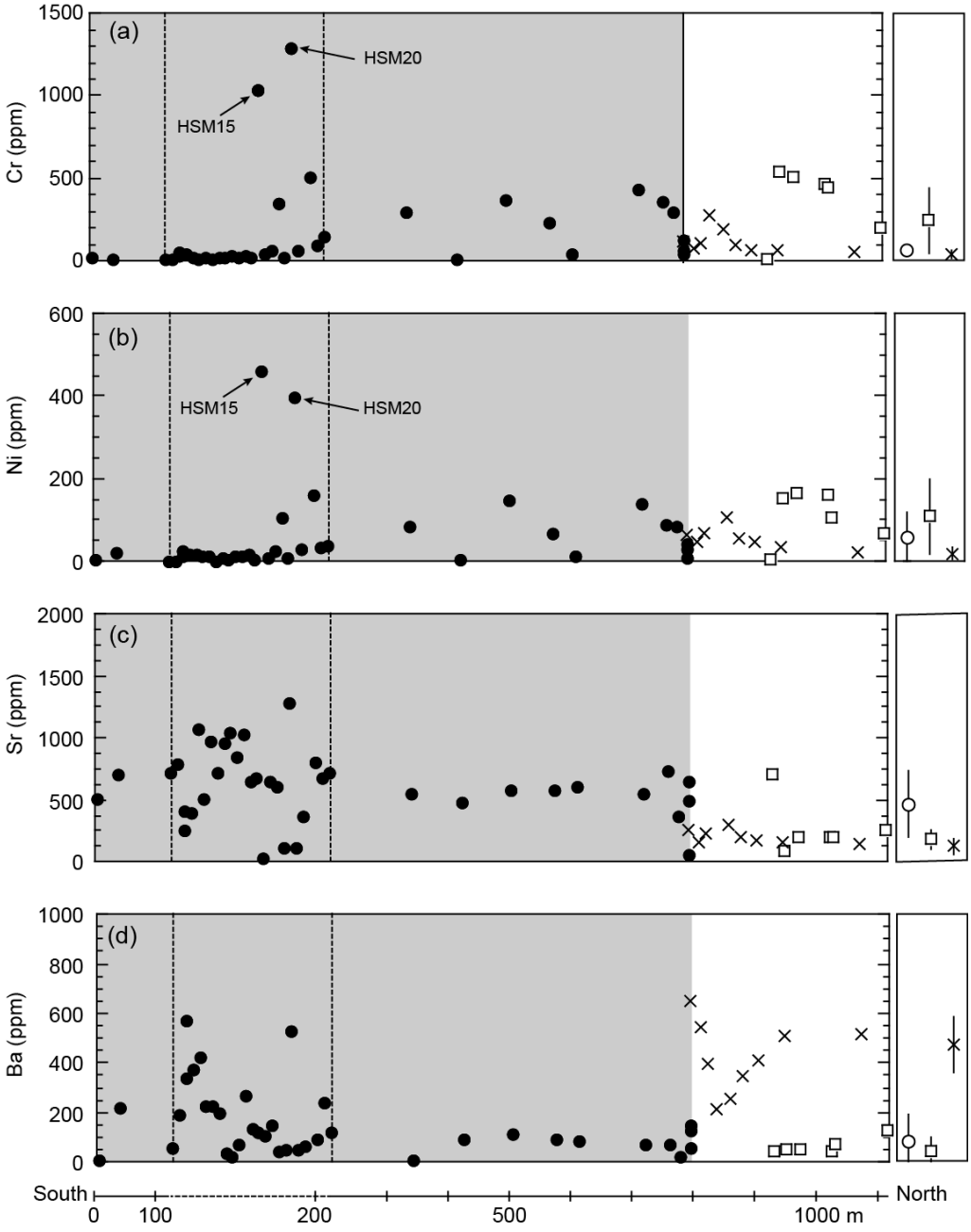

Fig. 12. Variations in (a) Cr, (b) Ni, (c) Sr, and (d) Ba concentrations (in ppm) of the Tonaru epidote-amphibolites along the Kokuryo River. Data sources are: Tonaru epidote-amphibolites (this study), Iratsu and Seba epidote-amphibolites (Aoya *et al*., 2006; Utsunomiya *et al*., 2011; Endo *et al*., 2012; Enami, unpublished data), basic schists (Okamoto *et al*., 2000; Nozaki *et al*., 2006; Utsunomiya *et al*., 2011; Enami, unpublished data), and pelitic schists (Goto *et al*., 1996; Kiminami and Ishihama, 2003; Aoya *et al*., 2006; Kiminami, 2010; Utsunomiya et al., 2011; Enami, unpublished data).

Sample HSM09, which was collected from around a layer of marble (Fig. 2b), has an unusually high X_{CaO} value of 0.97 (Fig. 11d). Samples HSM15, HSM18, and HSM20 have unusually low Al_2O_3 concentrations, less than 10 wt% (Fig. 11b). These samples are mostly composed of mafic phases and the modal compositions of their amphiboles are > 80–90 vol% (Fig. 11d). The variations in whole-rock compositions of major elements exhibit close relationships with the characteristics of observed mineral assemblages and compositions. SiO_2-rich samples contain large amounts of quartz and/or plagioclase. Most of the garnet-bearing epidote-amphibolites, which occur at the southern and northern margins of the Tonaru body, tend to have higher FeO*/MgO values (2.03 ± 0.51) and MnO contents (0.18 ± 0.03wt%) than the garnet-free HSM (1.60 ± 0.58, 0.13 ± 0.03wt%) and TO (0.90 ± 0.56, 0.13 ± 0.05wt%) series (Supplementary Table S2). The garnet usually has a higher Fe^{2+}/Mg and Mn/Mg partitioning coefficient than the coexisting mafic silicate minerals (Thompson, 1976a, b; Loomis and Nimick, 1982; Hall, 1985). Therefore, the high FeO*/MgO and/or MnO-rich whole-rock compositions probably stabilized the garnet. A miscibility gap in the calcic amphibole system has been postulated under low- to medium-grade conditions, and it is well known that calcic amphibole with lower X_{Mg} values are distinctly more aluminous than coexisting higher X_{Mg} calcic amphibole (Robinson *et al.*, 1982). This fact suggests that decreasing X_{Mg} values promote selective substitutions of tschermakite and/or edenite compositions into calcic amphibole. Occurrences of Si-poor calcic amphiboles in the southern and northern regions of the Tonaru body probably resulted from lower X_{Mg} values of whole-rock compositions (Figs. 9 and 10). Minor occurrences of biotite in limited (Table 1) are also considered to be an effect of

concentrations. These values are similar to the three samples collected near the southern
and northern margins of the Tonaru body (TO0801, TO01, and TO16: Cr = 16–295 ppm, Ni = 5–85 ppm, Sr = 363–702 ppm, and Ba = 9–220 ppm) and the Iratsu and Seba epidote-amphibolites (Cr = 5–279 ppm, Ni = 1–175 ppm, Sr = 24–1194 ppm, and Ba = 1–494 ppm). Chromium and Ni concentrations in most samples collected near the southern and northern margins (TO0801, TO01, HSM series, and TO16) are generally less than 100 and 40 ppm, respectively. However, extremely Cr- and Ni-rich samples sporadically occur within the southern marginal zone (HSM15, HSM18, HSM20, and HSM23: Cr = 347–1291 ppm and Ni = 108–460 ppm). Strontium and Ba concentrations in the HSM series and TO16 (Sr = 5–1277 ppm and Ba = 8–570 ppm) are more variable than those of the other nine samples in the TO series.

6.1.2 Shear zone

The basic layer (TOCA01 and 02) and basic lens (TOCV) of the shear zone have compositions that are richer in SiO_2 (up to 53.9 wt%), higher in FeO*/MgO (up to 2.43), and lower in X_{CaO} (as low as 0.62) relative to the other nine samples directly to the south (TO0801, TO01, and TO07-TO2508) (Supplementary Table S3). Sample TOCV is distinctly poorer in Sr (58 ppm) and Ba (55 ppm) than TOCA01 and 02 (Sr, 497 and 656 ppm, Ba, 125 and 150 ppm, respectively). The pelitic lense has major and trace element compositions similar to the pelitic schists from the Kokuryo River route and other areas of the Sanbagawa belt (Figs. 11 and 12).

6.1.3. Metapelite and basic schists

Tonaru metapelites on the northern side of the Tonaru body have similar SiO_2 (65.8 ± 2.8 wt%) and Al_2O_3 (15.1 ± 0.9 wt%) concentrations and FeO*/MgO (2.05 ± 0.64) values (Fig. 6; Supplementary Table S4) to those of other Sanbagawa pelitic schists (SiO_2 = 68.8 ± 3.8 wt%, Al_2O_3 = 15.2 ± 1.6 wt%, and FeO*/MgO = 2.49 ± 0.35) reported in literature (cf. figure caption of Fig. 11). In contrast, X_{CaO} values of the Tonaru pelitic schists tend to increase toward the boundary with epidote-amphibolites from 0.12 to 0.41 and are higher than the average value of other Sanbagawa pelitic schists (0.14 ± 0.11). The Tonaru pelitic schists are characteristically richer in Cr (116 ± 73 ppm) and Ni (65 ± 38 ppm) than previously analyzed Sanbagawa pelitic schists (Cr = 46 ± 26 ppm and Ni = 19 ± 14 ppm: Fig. 7; Supplementary Table S4).

Tonaru basic schists on the northern side of the Tonaru body and pelitic schists contain SiO_2 (47.9 ± 3.3 wt%) and Al_2O_3 (17.2 ± 1.4 wt%) concentrations (Fig. 11; Supplementary Table S5) similar to those of other Sanbagawa basic schists (i.e., SiO_2 = 47.0 ± 2.8 wt% and Al_2O_3 = 15.4 ± 1.8 wt%) reported in the literature. However, their FeO*/MgO (1.98 ± 0.67) and X_{CaO} (0.70 ± 0.10) values tend to be higher and lower, respectively, than the other Sanbagawa basic schists with FeO*/MgO =1.69 ± 0.46 and X_{CaO} = 0.80 ± 0.07, which are reported in literature. Chromium, Ni, and Sr contents are variable: 14–542 ppm, 6–164 ppm, and 90–700 ppm, respectively (Fig. 12 and Supplementary Table S5).

6.2. REE compositions

Figure 13 shows the REE patterns of the epidote-amphibolites and basic and pelitic lenses in the shear zone. The REE pattern of the pelitic lens shows a combination of a

steep slope in light (L)REE and a flat slope for heavy (H)REE. This REE pattern is similar to those of reference sedimentary rocks, such as the North American Shale Composite (NASC; McLennan, 1989) and the Post Archean Australian Shale (PAAS; McLennan, 1989). The epidote-amphibolites display three types of REE patterns which are totally different from each other according to the locations of these epidote-amphibolite. The HSM series samples are LREE enriched, as indicated by their steep patterns from LREE to HREE. The basic lens (TOCV) from the shear zone displays a flat pattern and is relatively enriched in HREE when compared to other Tonaru samples. Samples TO07 and TO10 have lower REE concentrations than the other Tonaru epidote-amphibolites and produce REE patterns with a gentle slope and slight enrichment in LREE.

7. DISCUSSION

The origin of the protoliths of the Sanbagawa metamorphic rocks in the Besshi and surrounding areas has been investigated based on geochemical studies by many scientists. For example, Okamoto *et al.* (2000), Nozaki *et al.* (2006), Utsunomiya *et al.* (2011), Uno *et al.* (2014) and so on. Utsunomiya *et al.* (2011) considered that the igneous protoliths of the Iratsu epidote-amphibolies, and eclogites, hereafter referred to Tonaru samples. Samples TO07 and TO10 have lower REE concentrations than the other Tonaru epidote-amphibolites and produce REE patterns with a gentle slope and slight enrichment in LREE.

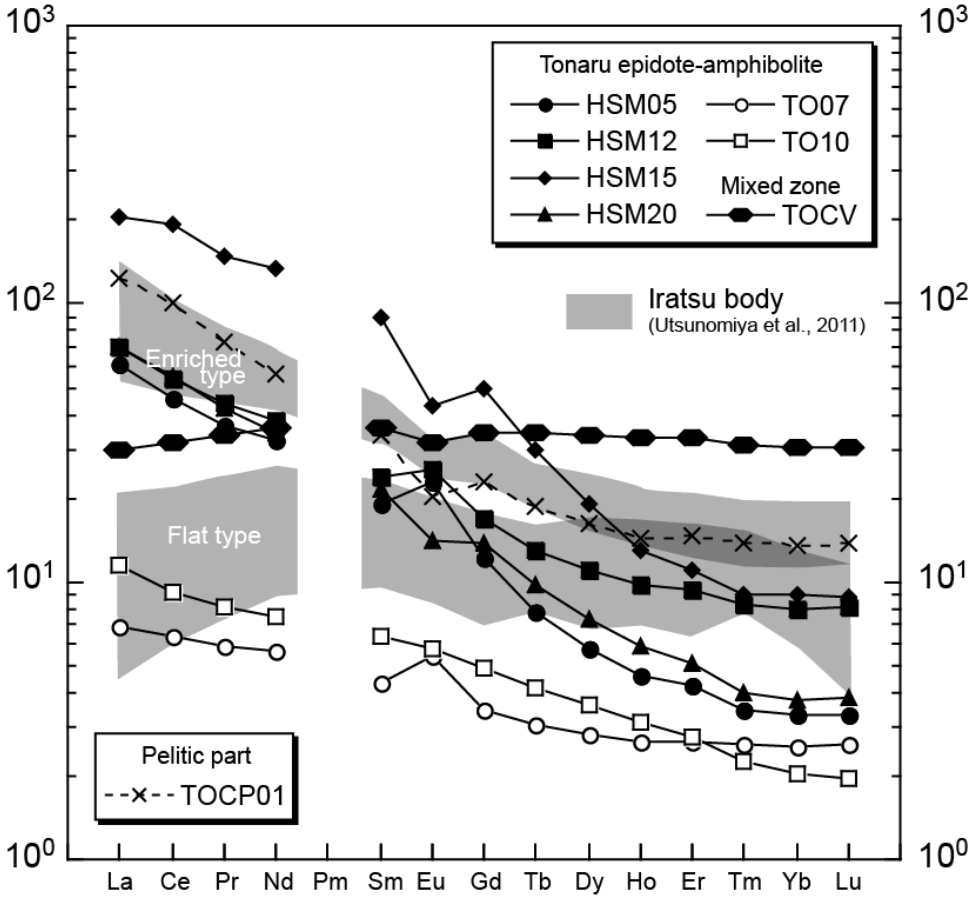

Fig. 13. REE patterns of the Tonaru epidote-amphibolites and a pelitic schist compared with those from the Iratsu epidote-amphibolites reported by Utsunomiya *et al*. (2011). C1 chondrite values are from Sun and McDonough (1989).

8. DISCUSSION

The origin of the protoliths of the Sanbagawa metamorphic rocks in the Besshi and surrounding areas has been investigated based on geochemical studies by many scientists. For example, Okamoto *et al.* (2000), Nozaki *et al.* (2006), Utsunomiya *et al.* (2011), Uno *et al.* (2014) and so on. Utsunomiya *et al.* (2011) considered that the igneous protoliths of the Iratsu epidote-amphibolies, and eclogites, hereafter referred to as the epidote-amphibolites as a group unless otherwise stated, were parts of the middle-lower crust of an oceanic island arc that had probably not undergone severe seawater alteration prior to the Sanbagawa metamorphism. These conclusions were based on analysis of trace elements, REEs, and Sr-Nd isotopic data. Utsunomiya *et al.* (2011) also reported that the Iratsu epidote-amphibolites exhibit two distinct REE patterns of LREE, enriched and flat, although the HREE patterns of all samples are nearly flat. Considering that the LREE-enriched rocks have relatively lower $\varepsilon_{Nd}(t)$ (−1 to +1.5) values than the rocks with flat REE patterns (ε_{Nd} (t) = +1.5 to +4), they argued that the protoliths of the Iratsu epidote-amphibolites were generated by mixing of two components, which are enriched and depleted in high field strength elements (HFSE), respectively.

The Sanbagawa basic schists have chemical characteristics similar to normal (N-) or enriched (E-) mid-ocean-ridge basalt (MORB) and are chemically and petrographically distinguishable from the Iratsu epidote-amphibolites (Okamoto *et al.*, 2000; Nozaki *et al.*, 2006; Utsunomiya *et al.*, 2011; Uno *et al.*, 2014). Utsunomiya *et al.* (2011) suggested that protoliths of the basic schists likely formed in a plume-influenced mid-ocean ridge or back-arc basin. Pelitic schists surrounding the Iratsu

epidote-amphibolites have evolved continental geochemical signatures, consistent with their origin as continent-derived trench-fill turbidites (Utsunomiya *et al.*, 2011). These data suggest that the protoliths of the Sanbagawa metamorphic rocks formed in a variety of tectonic settings (Utsunomiya *et al.*, 2011).

7.1. Compositional heterogeneity of epidote-amphibolite

The epidote-amphibolites of the Tonaru body show a wide range of major and trace elements compositions. Figures 14 and 15 compare representative compositional characteristics of the Tonaru epidote-amphibolites with those of the Iratsu and Seba epidote-amphibolites and the Sanbagawa basic and pelitic schists. These figures show that the Iratsu and Seba epidote-amphibolites and basic schists have similar compositional ranges except on the Ti/100–Zr-Sr/2 diagram (Fig. 15a), which implies that the epidote-amphibolites generally have a higher proportion of Sr (Sr/2 : Ti/100 : Zr = 69.2 ± 17.0 : 18.0 ± 10.1 : 12.8 ± 10.5) than the basic schists (Sr/2 : Ti/100 : Zr = 33.9 ± 9.8 : 34.4 ± 5.6 : 31.7 ± 7.0). In contrast, the Tonaru epidote-amphibolites have wider compositional ranges, and some of the HSM series samples show intermediate compositions between the basic lithologies and pelitic schists. The Tonaru epidote-amphibolites exhibit variable REE patterns (Fig. 13). Samples TO07 and TO10 have REE patterns similar to the LREE-enriched pattern of the Iratsu likely petrologically and geochemically metamorphosed layered gabbros, as has been

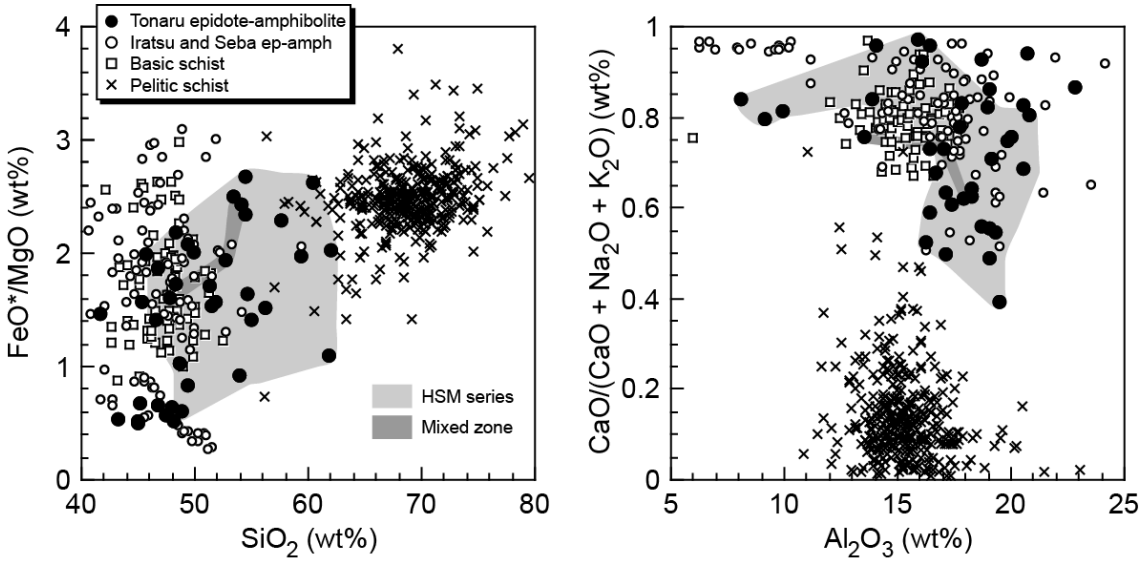

Fig. 14. Comparisons of selected major elements of the Tonaru and Iratsu epidote amphibolites, basic schists, and pelitic schists in (a) SiO2–FeO*/MgO and (b) Al2O3-CaO/(CaO + Na2O + K2O) diagrams. Data sources are: Tonaru epidote-amphibolites (this study), Iratsu and Seba epidote-amphibolites (Goto and Banno, 1990; Aoya *et al*., 2006; Utsunomiya *et al*., 2011; Endo *et al*., 2012; Weller *et al*., 2015; Enami, unpublished data), basic schists (Banno, 1964; Ernst *et al*., 1970; Okamoto *et al*., 2000; Nozaki *et al*., 2006; Utsunomiya *et al*., 2011; Enami, unpublished data), and pelitic schists (Banno, 1964; Ernst et al., 1970; Goto et al., 1996; Kiminami and Ishihama, 2003; Aoya et al., 2006; Kiminami, 2010; Fujiwara et al., 2011; Utsunomiya et al., 2011; Enami, unpublished data). Some data for basic schists with SiO_2< 40 wt% were omitted.

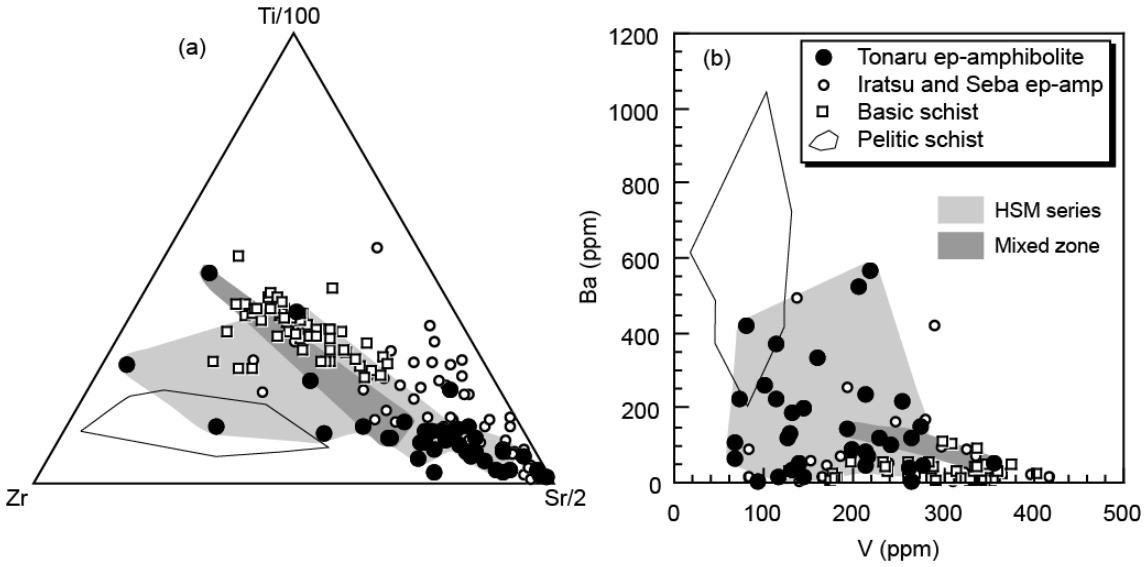

Fig. 15. Comparisons of selected trace elements of the Tonaru and Iratsu epidote amphibolites, basic schists, and pelitic schists (a) Ti/100-Zr-Sr/2 and (b) V-Ba diagrams. Data sources are: Tonaru epidote-amphibolites (this study), Iratsu and Seba epidote-amphibolites (Aoya *et al*., 2006; Utsunomiya *et al*., 2011; Endo *et al*., 2012; Enami, unpublished data), basic schists (Okamoto *et al*., 2000; Nozaki *et al*., 2006; Utsunomiya *et al*., 2011; Enami, unpublished data), and pelitic schists (Goto *et al*., 1996; Kiminami and Ishihama, 2003; Aoya *et al*., 2006; Kiminami, 2010; Utsunomiya *et al*., 2011;Enami, unpublished data).

commonly hypothesized (Banno *et al.*, 1976; Kunugiza *et al.*, 1986; Takasu, 1989). Utsunomiya *et al.* (2011) described the Iratsu epidote-amphibolites as being comparable in composition to the accreted and exposed middle-lower crustal rocks of some paleo-island arc sections in $(Ti/Gd)_{PM}$–$(Zr/Sm)_{PM}$ plots, where the subscript PM indicates ratios of values normalized to the primitive mantle (Fig. 16). Samples TO07 and TO10, which are considered to be metagabbro, have distinctly higher $(Zr/Sm)_{PM}$ values and slightly lower $(Ti/Gd)_{PM}$ values than most of the Iratsu samples, similar to middle crustal rocks, according to the criteria proposed by Utsunomiya *et al.* (2011).

The HSM series, which were collected from the southern margin, probably record the influence of compositional modification and introduction of sedimentary components. Many processes following protolith formation, including dehydration during metamorphism to hydration during exhumation, could have modified the whole-rock compositions. Seawater alteration might also be a major process of compositional modification of an oceanic plate and related lithologies prior to subduction (Verma, 1992; Gibson *et al.*, 1996). However, Utsunomiya *et al.* (2011) considered that evidence of severe seawater alteration is not discernible in the Iratsu epidote-amphibolite body. Additionally, seawater alteration is probably incapable of introducing a sedimentary signature into the basic lithologies. Fujiwara *et al.* (2011) systematically analyzed whole rock compositions of pelitic schists from the whole-grade zones in the Asemi-gawa region of the Sanbagawa belt and concluded that the Sanbagawa metamorphic rocks did not experience significant dissolution and/or addition of major elements by dehydration recrystallization during prograde metamorphism. Therefore, two other major processes remain as potential mechanisms in the formation of the intermediate compositions between the gabbroic and pelitic lithologies: (1) infiltration of metamorphic fluid and

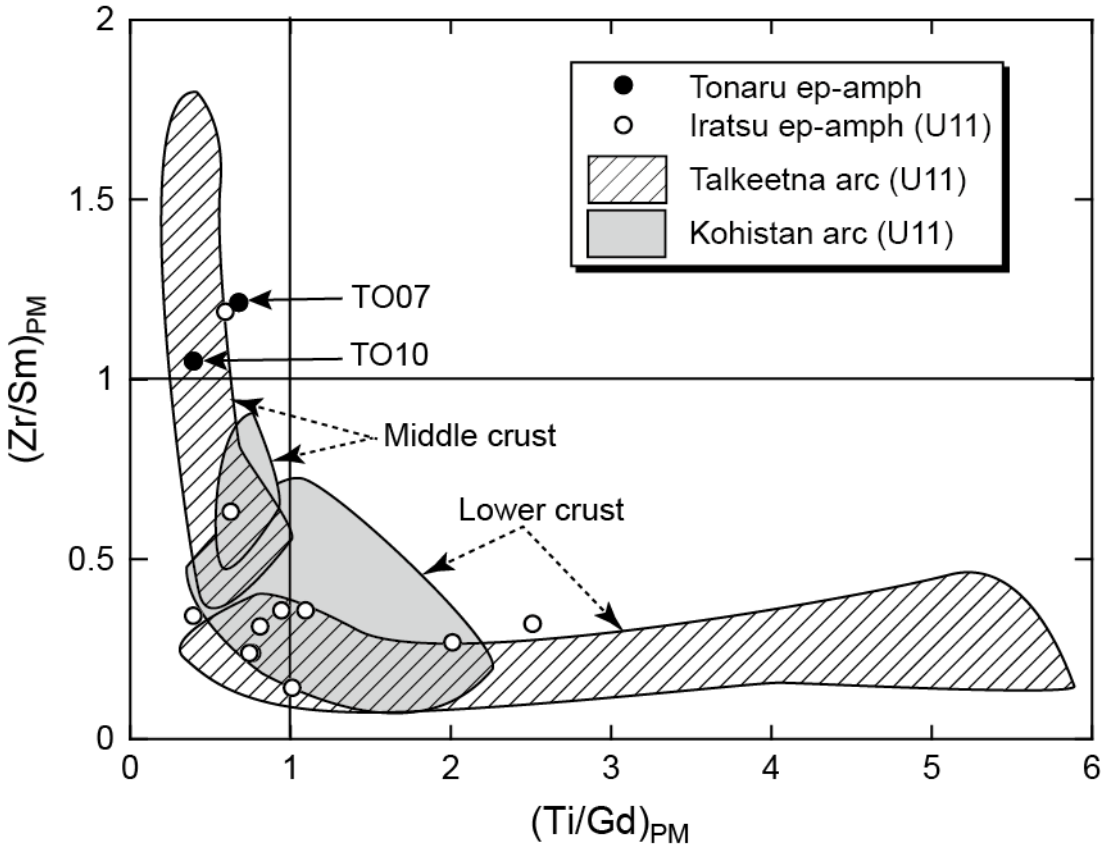

Fig. 16. A comparison of Tonaru and Iratsu epidote-amphibolites and the lower and middle crust of paleo-ocean island arc sections on the (Zr/Sm)PM-(Ti/Gd)PM diagram proposed by Utsunomiya et al. (2011). For Tonaru data, two samples of TO 07 and 10, which are considered to be metamorphosed layered gabbro by textural and compositional characteristics, were selectively plotted. PM indicates ratios of values normalized to primitive mantle compositions from Sun and McDonough (1989). Abbreviation U11 is from Utsunomiya et al. (2011).

metasomatic transfer or introduction of elements into the metagabbroic lithologies from the surrounding sedimentary lithologies; and (2) mixing of these two lithologies promoted by sedimentary processes at the protolith formation stage and/or mechanical processes during subduction or exhumation.

Uno *et al.* (2014) showed that the HFSE and REE compositions and Sr-Nd-Pb isotopic ratios of the Sanbagawa basic schists in the Asemi-gawa region in the lower-grade chlorite zone are different from those in the garnet and higher-grade zones, and concluded that the Sanbagawa schists have undergone significant hydration during decompression towards the surface at the final stage of metamorphism. Figure 8b shows a multi-element spidergram (Pearce, 1983) of the Iratsu and Tonaru epidote-amphibolites normalized by average compositions of the Iratsu eclogites (6 samples) reported by Utsunomiya *et al.* (2011). The Iratsu epidote-amphibolites show two types of patterns: (1) five of six samples have flat patterns except for the distinct depletion of Th; and (2) epidote-amphibolite (S09) is noticeably enriched in fluid mobile elements (K, Rb, and Ba) and incompatible elements (Th, Ta, and Nb). The Tonaru epidote-amphibolites have Rb-rich compositions similar to sample S09 from the Iratsu body. Therefore, infiltration of metamorphic fluid has probably influenced whole-rock compositions, especially with respect to the fluid mobile elements of the Tonaru epidote-amphibolites and some Iratsu epidote-amphibolites. This phenomenon occurred during their formation stage by the process of hydration of the original eclogites, as well as due to extensive hydration after epidote-amphibolite facies recrystallization during the final exhumation to the Earth's surface, as concluded by Uno *et al.* (2014). However, it is difficult to explain the simultaneous increase in SiO_2 (Fig. 11a), spikes in the concentrations of Cr (Fig. 12a) and Ni (Fig. 12b), and local

depletion in Al_2O_3 (Fig. 11b) observed in some samples of the HSM series on the basis of the fluid infiltration process. Lithological mixing is a more viable process in explaining the compositional characteristics of the HSM series samples. Pelitic lenses occur in epidote-amphibolites in the river floor of the Kokuryo River, and the host epidote-amphibolites have more siliceous compositions than the other epidote-amphibolites (Miyagi and Takasu, 2005). These data support the notion of lithological mixing occurring around the Tonaru epidote-amphibolites, although the outcrops on the valley floor were inaccessible and we did not observe them along the survey route. Two possible stages are hypothesized for the lithological mixing: (1) during subduction and metamorphism; and (2) during protolith formation before subduction. In the subduction stage, lithological mixing might have progressed due to a mechanical process. However, it is not conclusive that the mechanical mixing process generally causes compositional homogenization of the mixed lithologies. For example, compositional homogenization process at the lithological boundary by mechanical interaction might have been generally limited as discussed in the next section, and thus, the mechanical mixing model cannot fully explain the 80–90 m wide zone of compositional heterogeneity in the epidote-amphibolites at the southern margin of the Tonaru body (the HSM series). The layer of marble, which is intercalated concordantly or subconcordantly in the host epidote-amphibolites (Fig. 2c), might also be inconsistent with a mechanical mixing model. The compositional heterogeneities of the HSM series samples can be attributed to sedimentary mixing of basic and sedimentary materials during the formation of their protolith. High-concentrations of Cr and Ni in some samples (Fig. 12a, b) suggest local addition of ultramafic materials related to sedimentary mixing.

7.2. Pelitic rocks

The zonal structure of garnet in Besshi region, central Shikoku has been investigated by Kouketsu, *et al* (2014), and they reported that garnets grains in the Besshi region, central shikoku, usually show chemically composite zoning with resolved inner and outer segments, respectively. The inner segments usually contains paragonite, and the outer segments rarely includes albite but no paragonite. For this composite-zoned garnet imply the following successive metamorphic path: prograde eclogite facies stage→ decompression and hydration reaction stage→prograde epidote→amphibolite facies stage. The garnet from the pelitic rocks of the Tonaru mass belongs to the composite-zoned garnet, and the pelitic rocks contain composite zoned garnet with paragonite inclusions, and have probably recrystallized under eclogite facies conditions along with the Tonaru body. This evidence suggests that mechanical mixing of gabbroic and pelitic lithologies developed before or during eclogite facies subduction zone.

7.3. Formation of shear zone and compositional characteristic at lithologic boundary

Petrographic and compositional characteristics of the TOC series from the shear zone at the northern margin might have recorded mechanical mixing processes during the formation of the shear zone. The shear zone and the surrounding Tonaru epidote-amphibolite and Tonaru pelitic sand basic schists contains sodic plagioclase ($An_{10–20}$), suggesting that they belong to the oligoclase-biotite zone and shares the results of prograde epidote-amphibolite facies metamorphism (Enami, 1982). Therefore, the formation of the shear zone certainly occurred prior to or during the prograde

epidote-amphibolite facies stage (Supplementary Fig. S1). Symplectitic pseudomorphs after omphacite was rarely observed in the epidote-amphibolites

along the Kokuryo River route (Moriyama, 1990; Miyagi and Takasu, 2005). Complex zoned garnet (Supplementary Fig. S3) additionally suggests that these samples have experienced prograde eclogite facies and subsequent prograde epidote-amphibolite facies metamorphism (Supplementary Fig. S1). It is still uncertain whether lithologies of the shear zone and the adjoining Tonaru pelitic and basic schists belong to the eclogite unit. If the shear zone has experienced eclogite facies recrystallization, its formation is considered to date back to the eclogite facies stage or before (Supplementary Fig. S1). Alternatively, if the shear zone and the Tonaru pelitic and basic schists did not record the eclogite facies metamorphism, the juxtaposition of eclogite and non-eclogite units and the formation of shear zone progressed during the prograde epidote-amphibolite faces stage (Supplementary Fig. S1).

Two types of basic lithologies occur in the shear zone, one as a layer bordering the Tonaru body (TOCA01 and 02), and the other a lens in the matrix of basic-pelitic alternation (TOCV). Although these samples generally show a similar range of major and trace element compositions to each other (Figs. 11a, b and 12b), these samples could be distinguished on the Ti/100–Zr-Sr/2 diagram (Fig. 15a). The basic layer (TOCA01 and 02) has high Sr/2 proportions (63.0 and 64.1%) corresponding to the Iratsu and Seba epidote-amphibolites (69.2 ± 17.0%), which probably suggests that the basic layer was the sheared member of the Tonaru epidote-amphibolite. On the other hand, the basic lens (TOCV) has a low Sr/2 proportion (10.1%) similar to the Sanbagawa basic schists (33.9 ± 9.8%). The REE pattern of TOCV is similar to the flat to slightly LREE-depleted pattern of the Sanbagawa basic schists, the protolith of which

is considered to be N-MORB (Okamoto et al., 2000; Nozaki et al., 2006; Utsunomiya et al., 2011; Uno et al., 2014). These data imply that a substantial lithologic boundary probably occurs between the basic layer (TOCA01 and 02) and fine alternating layers of basic and pelitic lithologies within the shear zone.The shear zone is narrow (1.5–2.5 m in width), and sample TO16, which was collected 6–7 m from the pelitic schist, shows no critical evidence supporting the influence of pelitic components (Supplementary Tables S2 and S3). Additionally, there is no conclusive data suggesting compositional interaction along the lithologic boundary between the basic layer (TOCA01 and 02) and the basic-pelitic alternating lithologies, including samples TOCA and TOCP01. These facts suggest that the assumed mechanical mixing at the lithologic boundaries was not extensive and might not have effectively altered the compositions of metamorphic rocks during the shearing process, as exemplified along the Kokuryo River route. Consequently, obvious alteration of whole-rock compositions during metamorphism, such as changes that can be discussed based on major element characteristics, might not generally progress without effective element transportation by metamorphic fluid, except for some particular cases such as formation and interfusion of rock powder during mylonitization. In the case of basic-basic rock and pelitic-basic rock pairs discussed here, these lithologies probably experienced similar dehydration and hydration reactions during prograde and retrograde stages, respectively. During prograde metamorphism, the released metamorphic fluid from basic and/or pelitic rocks might have not infiltrated and chemically altered the adjacent lithologies. This might be different from the case of chemical interaction between dehydrated slab and hydrated wedge mantle of regional scale and/or pelitic/basic rocks and ultrabasic rock of outcrop

scale. Consequently, chemical interactions at the interfaces of basic-basic rocks and pelitic-basic rocks are probably interactions at the interfaces of basic-basic rocks and pelitic-basic rocks are probably hard to effectively progress during prograde metamorphism.

9. CONCLUSIONS

Petrographic and geochemical characteristics of the Tonaru epidote-amphibolites and the surrounding pelitic and basic schists were discussed based on their major and trace element compositions, including REEs. Most of the samples from the Tonaru body are metamorphosed layered gabbro. Samples from the southern marginal zone (80–90 m wide) exhibit various major and trace element compositions suggesting that their protoliths are a mixture of mafic, ultramafic, and/or sedimentary lithologies.

A shear zone, developed at the boundary between the Tonaru body and pelitic schists on its northern boundary, is composed of a basic layer and fine alternating layers of basic and pelitic bands with lenses. The basic layer and basic lens show compositional characteristics in common with the Tonaru epidote-amphibolites of metagabbro and Sanbagawa basic schists, respectively, suggesting that the boundary of protoliths corresponds to that between the basic and alternating layers. There is no petrographic or geochemical evidence implying any interaction between the adjoining two lithologies during formation of the shear zone. This fact might suggest that a simple mechanical mixing process does not generally result in chemical modification of rocks on scales of tens of cm without any effective involvement of metamorphic fluid. On the other hand, the pelitic rocks contain composite zoned garnet with paragonite inclusions, and have probably recrystallized under eclogite facies conditions along with the Tonaru body.

This evidence suggests that mechanical mixing of gabbroic and pelitic lithologies developed before or during eclogite facies subduction zone.

ACKNOWLEDGEMENTS

I would like to express my sincere thanks to all those who have been given me all the support of my study in Nagoya University.

First of all, I would like to express my heartfelt gratitude to Professor Masski Enami, my supervisor, to accept me as a graduate student, and also gave me his constant encouragement and guidance during my stay in Nagoya University.

My supervisor also gave me many chances to attend the academic conferences, and I benefit a lot from these conferences. I also deeply appreciate my supervisor that let me have a chance to work as a research assistant for a long time in Petrology lab in my doctoral course, and this part time job gave me a whole of financial supports in Japan. These financial supports make me concentrate on my research and finish my doctoral course successfully.

I also would like to thank Professor Simon Wallis, Tokyo University, Professor Katsuyoshi Michibayashi, Professor Takenori Kato, Nagoya University and Assistant Professor Yui Kouketsu, Nagoya University who gave me a lot of appropriate advice about my presentations in the Ganko meetings.

A special thank to Professor Motohiro Tsuboi, Kwansei Gakuin University, a very friendly teacher, helped me a lot in my fieldwork and laboratory work, and his student Yuki Wakasugi, Kwansei Gakuin University, also gave me valuable advices on laboratory work and helped me make some experiments in Kwansei Gakuin University.

Finally, I would like to express my sincere thanks to fellow colleagues from Petrology Lab because they taught me not only how to use all of the facilities in our Lab, but also a lot of Japanese culture since I am a foreign student. These valuable experiences will be helpful in the future.

REFERENCES

Aoki, K., Kitajima, K., Masago, H., Nishizawa, M., Terabayashi, M., Omori, S., Yokoyama, T., Takahata, N., Sano, Y. and Maruyama, S. (2009) Metamorphic *P-T*-time history of the Sanbagawa belt in central Shikoku, Japan and implications for retrograde metamorphism during exhumation. *Lithos* **113**, 393-407.

Aoya, M. (2001) *P-T-D* path of eclogite from the Sambagawa belt deduced from combination of petrological and microstructural analyses. *J. Petrol.* **42**, 1225-1248.

Aoya, M., Tsuboi, M. and Wallis, S. R. (2006) Origin of eclogitic metagabbro mass in the Sambagawa belt: Geological and geochemical constraints. *Lithos* **89**, 107-134.

Banno, S. (2004) Brief history of petrotectonic research on the Sanbagawa Belt, Japan. *Isl. Arc*. **13**, 475-483.

Banno, S., Yokoyama, K., Enami, M., Iwata, O., Nakamura, K. and Kasashima, S. (1976) Petrology of the peridotite-metagabbro complex in the vicinity of Mt. Higashi-akaishi, Central Shikoku. Part I. Megascopic textures of the Iratsu and Tonaru epidote amphibolite masses. *Sci. Rep. Kanazawa Univ.* **21**, 139-159.

Banno, S., Yokoyama, K., Iwata, O. and Terashima, S. (1976) Genesis of epidote amphibolite masses in the Sanbagawa metamorphic belt of central Shikoku. *J. Geol. Soc. Japan*. **82**, 199-210 (in Japanese with English abstract).

Chen, R.-X., Li, H.-Y., Zheng, Y.-F., Zhang, L., Gong, B., Hu, Z. and Yang, Y. (2017) Crust–Mantle Interaction in a Continental Subduction Channel: Evidence from Orogenic Peridotites in North Qaidam, Northern Tibet. J. Petrol. **58**, 191-226.

Enami, M. (1982) Oligoclase-biotite zone of the Sanbagawa metamorphic terrain in the Bessi district, central Shikoku, Japan. *J. Geol. Soc. Japan*. **88**, 887-900 (in

Japanese with English abstract).

Enami, M. (1983) Petrology of pelitic schists in the oligoclase-biotite zone of the Sanbagawa metamorphic terrain, Japan: phase equilibria in the highest grade zone of a high-pressure intermediate type of metamorphic belt. *J. Metamorphic Geol.* **1**, 141-161.

Enami, M. and Banno, S. (1980) Zoisite-clinozoisite relations in low- to medium-grade high-pressure metamorphic rocks and their implications. *Mineral. Mag.* **43**, 1005-1013.

Enami, M., Nagaya, T. and Maw Maw Win. (2017) An integrated EPMA-EBSD study of metamorphic histories recorded in garnet. *Am. Mineral.* **101**, 192-204.

Enami, M., Wallis, S. R. and Banno, Y. (1994) Paragenesis of sodic pyroxene-bearing quartz schists: implications for the *P-T* history of the Sanbagawa belt. *Contrib. Mineral. Petrol.* **116**, 182-198.

Endo, S. (2010) Pressure-temperature history of titanite-bearing eclogite from the Western Iratsu body, Sanbagawa metamorphic belt, Japan. *Isl. Arc.* **19**, 313-335.

Endo, S., Mizukami, T., Wallis, S. R., Tamura, A. and Arai, S. (2015) Orthopyroxene-rich rocks from the Sanbagawa Belt (SW Japan): Fluid-rock interaction in the forearc slab-mantle wedge interface. *J. Petrol.* **56**, 1113-1137.

Endo, S. and Tsuboi, M. (2013) Petrogenesis and implications of jadeite-bearing kyanite eclogite from the Sanbagawa belt (SW Japan). *J. Metamorphic Geol.* **31**, 647-661.

Endo, S., Wallis, S. R., Tsuboi, M., Aoya, M. and Uehara, S. (2012) Slow subduction and buoyant exhumation of the Sanbagawa eclogite. *Lithos* **146**, 183-201.

Ernst, W. G., Seki, Y., Onuki, H. and Gilbert, M. C. (1970) Comparative study of low-grade metamorphism in the California coast ranges and the outer

metamorphic belt of Japan. *Geol. Soc. Am. Mem*, **124**, Geological Society of America, 276 pp.

Fujiwara, S., Yamamoto, K. and Mimura, K. (2011) Dissolution processes of elements from subducting sediments into fluids: evidence from the chemical composition of the Sanbagawa pelitic schists. *Geochem. J.* **45**, 221-234.

Gibson, I. L., Beslier, M.-O., Cornen, G., Milliken, K. L. and Seifert, K. E. (1996). Major- and trace-element seawater alteration profiles in serpentinite formed during the development of the Iberia margin, Site 897. In: *Proc. ODP, Sci. Results* (Whitmarsh, R. B., Sawyer, D. S., Klaus, A. and Masson, D. G. eds.), **149,** College Station, TX (Ocean Drilling Program), 519-527.

Goto, A. and Banno, S. (1990) Hydration of basic granulite to garnet-epidote amphibolite in the Sanbagawa metamorphic belt, central Shikoku, Japan. *Chem. Geol.* **85**, 247-263.

Goto, A., Higashino, T. and Sakai, C. (1996) XRF analyses of Sanbagawa pelitic schists in central Shikoku, Japan. *Mem. Fac. Sci. Kyoto Univ., Ser. Geol. Mineral.* **58**, 1-19.

Hall, R. P. (1985) Mg-Fe-Mn distribution in amphiboles, pyroxenes, and garnets and implications for conditions of metamorphism of high-grade early Archaean iron-formation, southern West Greenland. *Mineral. Mag.* **49**, 117-128.

Hara, I., Shiota, T., Hide, K., Okamoto, K., Takeda, K., Hayasaka, Y. and Sakurai, Y. (1990) Nappe structure of the Sambagawa Belt. *J. Metamorphic Geol.* **8**, 441-456.

Hattori, K., Wallis, S., Enami, M. and Mizukami, T. (2010) Subduction of mantle wedge peridotites: Evidence from the Higashi-akaishi ultramafic body in the Sanbagawa metamorphic belt. *Isl. Arc*. **19**, 192-207.

Higashino, T. (1990) The higher-grade metamorphic zonation of the Sambagawa metamorphic belt in central Shikoku, Japan. *J. Metamorphic Geol.* **8**, 413-423.

Higashino, T. (1990) Metamorphic zones of the Sambagawa metamorphic belt in central Shikoku, Japan. *J. Geol. Soc. Japan*. **96**, 703-718 (in Japanese with English abstract).

Itaya, T., Tsujimori, T. and Liou, J. G. (2011) Evolution of the Sanbagawa and Shimanto high-pressure belts in SW Japan: Insights from K-Ar (Ar-Ar) geochronology. *J. Asian Earth Sci.* **42**, 1075-1090.

Isozaki, Y. and Itaya, T. (1990) Chronology of Sangbagawa metamorphism. *J. Metamorphic Geol*., **8**, 401-411.

Jahn, B. M., Tsai, C. H., Wu, F. and Lo, C. H. (1999) Crust-mantle interaction induced by deep subduction of the continental crust: Geochemical and Sr-Nd isotopic evidence from post-collisional mafic-ultramafic intrusions of the northern Dabie complex, central China. *Chem. Geol.* **157**, 119-146.

Kabir, M. F. and Takasu, A. (2016) Jadeite-garnet glaucophane schists in the Bizan area, Sambagawa metamorphic belt, eastern Shikoku, Japan: significance and extent of eclogite facies metamorphism. *J. Metamorphic Geol.* **34**, 893-916.

Kabir, M. F., Takasu, A., Matsuura, H. and Kuraya, I. (2016) Amphiboles from the kyanite–garnet amphibolite in the Tonaru metagabbro mass, Sambagawa metamorphic belt, central Shikoku, Japan. *Geosci. Rep. Shimane Univ.* **34**, 31-39.

Kato, T. (2005) New accurate Bence-Albee α-factors for oxides and silicates calculated from the PAP correction procedure. *Geostand. Geoanal. Res.* **29**, 83-94.

Kiminami, K. (2010) Parentage of low-grade metasediments in the Sanbagawa belt, eastern Shikoku, Southwest Japan, and its geotectonic implications. *Isl. Arc*. **19**,

530-545.

Kiminami, K. and Ishihama, S. (2003) The parentage of low-grade metasediments in the Sanbagawa Metamorphic Belt, Shikoku, southwest Japan, based on whole-rock geochemistry. *Sedim. Geol.* **159**, 257-274.

Kouketsu, Y. and Enami, M. (2010) Aragonite and omphacite-bearing metapelite from Besshi region, Sambagawa belt in central Shikoku, Japan and its implication. *Isl. Arc*. **19**, 165-176.

Kouketsu, Y., Enami, M. and Mizukami, T. (2010) Omphacite-bearing metapelite from the Besshi region, Sambagawa metamorphic belt, Japan: Prograde eclogite facies metamorphism recorded in metasediment. *J. Mineral. Petrol. Sci.* **105**, 9-19.

Kouketsu, Y., Enami, M., Mouri, T., Okamura, M. and Sakurai, T. (2014) Composite metamorphic history recorded in garnet porphyroblasts of Sambagawa metasediments in the Besshi region, central Shikoku, Southwest Japan. *Isl. Arc*. **23**, 263-280.

Kugimiya, Y. and Takasu, A. (2002) Geology of the Western Iratsu mass within the tectonic melange zone in the Sambagawa metamorphic belt, Besshi district, central Shikoku, Japan. *J. Geol. Soc. Japan*. **108**, 644-662 (in Japanese with English abstract).

Kunugiza, K., Takasu, A. and Banno, S. (1986) The origin and metamorphic history of the ultramafic and metagabbro bodies in the Sanbagawa metamorphic belt. *Blueschists and Eclogites, Geol. Soc. Am. Mem.* (Evans, B. E. and Brown, E. H. eds.), 375-385.

Leake, B. E., Woolley, A. R., Arps, C. E. S., Birch, W. D., Gilbert, M. C., Grice, J. D., Hawthorne, F. C., Kato, A., Kisch, H. J., Krivovichev, V. G., Linthout, K., Laird,

J., Mandarino, J. A., Maresch, W. V., Nickel, E. H., Rock, N. M. S., Schumacher, J. C., Smith, D. C., Stephenson, N. C. N., Ungaretti, L., Whittaker, E. J. W. and Guo, Y. Z. (1997) Nomenclature of amphiboles: Report of the subcommittee on amphiboles of the International Mineralogical Association, commission on new minerals and mineral names. *Am. Mineral.* **82**, 1019-1037.

Loomis, T. P. and Nimick, F. B. (1982) Equilibrium in Mn-Fe-Mg aluminous pelitic compositions and the equilibrium growth of garnet. *Can. Mineral.* **20**, 393-410.

Marocchi, M., Mair, V., Tropper, P. and Bargossi, G. M. (2009) Metasomatic reaction bands at the Mt. Hochwart gneiss-peridotite contact (Ulten Zone, Italy): insights into fluid-rock interaction in subduction zones. *Mineral. Petrol.* **95**, 251-272.

Matsumoto, M., Wallis, S., Aoya, M., Enami, M., Kawano, J., Seto, Y. and Shimobayashi, N. (2003) Petrological constraints on the formation conditions and retrograde P-T path of the Kotsu eclogite unit, central Shikoku. *J. Metamorphic Geol.* **21**, 363-376.

Matsuura, H., Takasu, A. and Kabir, M. F. (2013) High-Mg garnets in kyanite garnet amphibolite from the Tonaru metagabbro mass in the Sambagawa metamorphic belt, Besshi district, central Shikoku, Japan. *Geosci. Rep. Shimane Univ.* **32**, 13-32.

McLennan, S. M. (1989) Rare earth elements in sedimentary rocks; influence of provenance and sedimentary processes. In: *Rev. Mineral* (Lipin, B. R. and McKay, G. A. eds.), 169-200, Mineralogical Society of America.

Miyagi, Y. and Takasu, A. (2005) Prograde eclogites from the Tonaru epidote amphibolite mass in the Sambagawa Metamorphic Belt, central Shikoku,

southwest Japan. *Isl. Arc*. **14**, 215-235.

Miyamoto, A., Enami, M., Tsuboi, M. and Yokoyama, K. (2007) Peak conditions of kyanite-bearing quartz eclogites in the Sanbagawa metamorphic belt, central Shikoku, Japan. *J. Mineral. Petrol. Sci.* **102**, 352-367.

Morishita, T. and Suzuki, K. (1993) XRF analyses of the Mitsuhashi granite in the Shitara area, Aichi Prefecture. *Bull. Nagoya Univ. Furukawa Muse.* **No. 9**, 77-90 (in Japanese with English abstract).

Moriyama, H. (1990) Two metamorphic paths in the Tonaru epidote amphibolite mass within the Sambagawa belt, Besshi district, central Shikoku. *Geol. Rep. Simane Univ.* **9**, 49-54 (in Japanese with English abstract).

Mouri, T. and Enami, M. (2008) Areal extent of eclogite facies metamorphism in the Sanbagawa belt, Japan: New evidence from a Raman microprobe study of quartz residual pressure. *Geology*. **36**, 503-506.

Nakazaki, M., Tsuboi, M., Kanagawa, K., Kato, T. and Suzuki, K. (2004) Quantitative chemical analysis of rocks with X-ray fluorescence analyzer XRF-1800. *Bull. Nagoya Univ. Muse.* **20**, 79-91.

Naohara, R. and Aoya, M. (1997) Prograde eclogites from Sambagawa basic schists in the Sebadani area, central Shikoku, Japan. *Mem. Fac. Sci. Engi., Shimane Univ., Ser. A*. **30**, 63-73 (in Japanese with English abstract).

Nozaki, T., Nakamura k., Awaji, S. and Kato, Y. (2006) Whole-rock geochemistry of basic schists from the Besshi area, Central Shikoku: Implications for the tectonic setting of the Besshi sulfide deposit. *Resour. Geol.* **56**, 423-432.

Okamoto, K., Maruyama, S. and Isozaki, Y. (2000) Accretionary complex origin of the Sanbagawa, high *P/T* metamorphic rocks, central Shikoku, Japan; layer-parallel

shortening structure and greenstone geochemistry. *J. Geol. Soc. Japan* **106**,70-86.

Okamoto, K., Shinjoe, H., Katayama, I., Terada, K., Sano, Y. and Johnson, S. (2004) SHRIMP U-Pb zircon dating of quartz-bearing eclogite from the Sanbagawa Belt, south-west Japan; implications for metamorphic evolution of subducted protolith. *Terra Nova* **16**, 81-89.

Onuki, H., Yoshida, T. and Suzuki, T. (1978) The Fujiwara mafic-ultramafic complex in the Sanbagawa metamorphic belt of central Shikoku; 1, Petrochemistry and rock-forming mineralogy. *J. Japan. Assoc. Min. Petr. Econom. Geol.* **73**, 311-322 (in Japanese with English abstract).

Ota, T., Terabayashi, M. and Katayama, I. (2004) Thermobaric structure and metamorphic evolution of the Iratsu eclogite body in the Sanbagawa belt, central Shikoku, Japan. *Lithos* **73**, 95-126.

Pearce, J. A. (1983) Role of the sub-continental lithosphere in magma genesis at active continental margins. *Continental basalts and mantle xenoliths* (Hawkesworth, C. J. and Norry, M. J. eds.), 230-249, Shiva Publications.

Planka, T. and Langmuir, C. H. (1998) The chemical composition of subducting sediment and its consequences for the crust and mantle. *Chem. Geol.* **145**, 325-394.

Robinson, P., Spear, F. S., Schumacher, J. C., Laird, J., Klein, C., Evans, B. W. and Doolan, B. L. (1982) Phase relations of metamorphic amphiboles: Natural occurrence and theory. In: *Amphiboles: Petrology and Experimetal Phase Relations. Rev. Mineral.* (Veblen, D. R. and Ribbe, P. H. eds.), 1-227.

Sakurai, T. and Takasu, A. (2009) Geology and metamorphism of the Gazo mass

(eclogite-bearing tectonic block) in the Sambagawa metamorphic belt, Besshi district, central Shikoku, Japan. *J. Geol. Soc. Japan.* 115, 101-121 (in Japanese with English abstract).

Stern, R. J. (2002) Subduction zones. *Rev. Geophys.* **4**0, 1012. doi:10.1029/2001RG000108.

Sugisaki, R., Kinoshita, T., Shimomura, T. and Ando, K. (1981) An automatic X-ray fluorescence method for the trace element analyses in silicate rocks. *J. Geol. Soc. Japan*. **87**, 675-688 (in Japanese with English abstract).

Sugisaki, R., Shimomura, T. and Ando, K. (1977) An automatic X-ray fluorescence method for the analysis of silicate rocks. *J. Geol. Soc. Japan*. **83**, 725-733 (in Japanese with English abstract).

Sun, S. S. and McDonough, W. F. (1989) Chemical and isotopic systematics of oceanic basalts: implications for mantle composition and processes. In: *Magmatism in the Ocean Basins* (Saunders, A. D. and Norry, M. J. eds.), 313-345, Blackwell Scientific Publications.

Suzuki, K., Enami, M., Maekawa, H., Kato, T. and Ueno, T. (2018) Late Cretaceous CHIME monazite ages of Sanbagawa metamorphic rocks from Nushima, Southwest Japan. *J. Mineral. Petrol. Sci.* **113**, 1-9.

Taguchi, T. and Enami, M. (2014) Coexistence of jadeite and quartz in garnet of the Sanbagawa metapelite from the Asemi-gawa region, central Shikoku, Japan. *J. Mineral. Petrol. Sci.* **109**, 169-176.

Takasu, A. (1984) Prograde and retrograde eclogites in the Sambagawa metamorphic belt, Besshi district, Japan. *J. Petrol.* **25**, 619-643.

Takasu, A. (1989) *P-T* histories of peridotite and amphibolite tectonic blocks in the

Sambagawa metamorphic belt, Japan. In: *The Evolution of Metamorphic Belts* (Daly, J. S., R.A., C. and B.W.D., Y. eds.), 533-538, Blackwell Scientific Publications.

Terabayashi, M., Okamoto, K., Yamamoto, H., Kaneko, Y., Ota, T., Maruyama, S., Katayama, I., Komiya, T., Ishikawa, A., Anma, R., Ozawa, H., Windley, B. F. and Liou, J. G. (2005) Accretionary complex origin of the mafic-ultramafic bodies of the Sanbagawa Belt, central Shikoku, Japan. *Inter. Geol. Rev.* **47**, 1058-1073.

Thompson, A. B. (1976) Mineral reactions in pelitic rocks: I. Prediction of *P-T-X*(Fe-Mg) phase relations. *Am. J. Sci.* **276**, 401-424.

Thompson, A. B. (1976) Mineral reactions in pelitic rocks: II. calculation of some *P-T-X*(Fe-Mg) phase relations. *Am. J. Sci.* **276**, 425-454.

Tsuchiya, S. and Hirajima, T. (2013) Evidence of the lawsonite eclogite facies metamorphism from an epidote-glaucophane eclogite in the Kotsu area of the Sanbagawa belt, Japan. *J. Mineral. Petrol. Sci.* **108**, 166-171.

Uno, M., Iwamori, H., Nakamura, H., Yokoyama, T., Ishikawa, T. and Tanimizu, M. (2014) Elemental transport upon hydration of basic schists during regional metamorphism: Geochemical evidence from the Sanbagawa metamorphic belt, Japan. *Geochem. J.* **48**, 29-49.

Utsunomiya, A., Jahn, B.-m., Okamoto, K., Ota, T. and Shinjoe, H. (2011) Intra-oceanic island arc origin for Iratsu eclogites of the Sanbagawa belt, central Shikoku, southwest Japan. *Chem. Geol.* **280**, 97-114.

Verma, S. P. (1992) Seawater alteration effects on REE, K, Rb, Cs, Sr, U, Th, Pb and Sr-Nd-Pb isotope systematics of Midocean Ridge Basalt. *Geochem. J.* **26**,

159-177.

Wada, H., Enami, M. and Yanagi, T. (1984) Isotopic studies of marbles in the Sanbagawa metamorphic terrain, central Shikoku, Japan. *Geochem. J.* **18**, 61-73.

Wallis, S. R., Anczkiewicz, R., Endo, S., Aoya, M., Platt, J. P., Thirlwall, M. and Hirata, T. (2009) Plate movements, ductile deformation and geochronology of the Sanbagawa Belt, SW Japan; tectonic significance of 89-88 Ma Lu-Hf eclogite ages. *J. Metamorphic Geol.* **27**, 93-105.

Wallis. S. (1998) Exhuming the Sanbagawa metamorphic belt; the importance of tectonic discontinuities. *J. Metamorphic Geol.* **16.** 83-95.

Wallis, S. and Aoya, M. (2000) A re-evaluation of eclogite facies metamorphism in SW Japan: Proposal for an eclogite nappe. *J. Metamorphic Geol.* **18**, 653-664.

Wallis, S. and Okudaira, T. (2016) Paired metamorphic belts of SW Japan: the geology of the Sanbagawa and Ryoke metamorphic belts and the Median Tectonic Line. In: *The Geology of Japan* (Moreno, T., Wallis, S., Kojima, T. and Gibbons, W. eds.), 101-124, The Geological Society.

Wallis, S., Takasu, A., Enami, M. and Tsujimori, T. (2000) Eclogite and related metamorphism in the Sanbagawa belt, Southwest Japan. *Bull. Resear. Insti. Nat. Sci., Okayama Univ. Sci.* **26**, 3-17.

Weller, O. M., Wallis, S. R., Aoya, M. and Nagaya, T. (2015) Phase equilibria modelling of blueschist and eclogite from the Sanbagawa metamorphic belt of southwest Japan reveals along-strike consistency in tectonothermal architecture. *J. Metamorphic Geol.* **33**, 579-596.

Whitney, D. L. and Evans, B. W. (2010) Abbreviations for names of rock–forming minerals. *Am. Mineral.* **95**, 185-187.

Yamamoto, K. and Morishita, T. (1997) Preparation of standard composites for trace element analysis by X-ray fluorescence. *J. Geol. Soc. Japan*. 1037-1045 (in Japanese with English abstract).

Yokoyama, K. (1974) Petrogenesis of the Higashi-akaishi peridotite and Iratsu epidote amphibolite. *Master thesis, Kanazawa University* 90 pp (unpublished).

Zaw Win Ko, Enami, M. and Aoya, M. (2005) Chloritoid and barroisite-bearing pelitic schists from the eclogite unit in the Besshi district, Sanbagawa metamorphic belt. *Lithos* **81**, 79-100.